

VILNIUS UNIVERSITY
LIFE SCIENCE CENTER

KAMILĖ KASPERAVIČIŪTĖ

Neurobiology master's study program II year student

Master's thesis

**DEVELOPMENT OF A MICROFLUIDIC CHIP FOR STUDYING GLIOMA
CELL ADHESION**

Work supervisor: dr. E.Andriukonis

Vilnius, 2024

Contents

INTRODUCTION.....	4
1. LITERATURE REVIEW	6
1.1 Glioma biology and cell adhesion mechanisms	6
1.2 Microfluidic technology in a neuronal cell research	7
1.3 Microfluidic chip models of the blood-brain-barrier for glioma research.....	10
1.4 Microfluidic chip surface adhesion modification methods	16
2. METHODOLOGY	18
2.1 Design and fabrication of the microfluidic chip	18
2.1.1 Mold modeling and 3D printing	18
2.1.2 PDMS casting	19
2.1.3 Preparation of COC.....	20
2.1.4 OSTE injection casting	21
2.2 Cell line and culture conditions	22
2.3 Preparation of microchip channel for glioma cell adhesion	22
2.4 Preparation of Glioma cell culture.....	23
2.5 Cell attachment and seeding in microchip.....	24
2.6 Microfluidic chip monitoring using a microscope and image capturing	24
2.7 Microfluidic technique	25
2.8 Statistical analysis.....	27
3. RESULTS	28
3.1 Microchip production methodology improvements	28
3.2 Microfluidic pump impact on glioma cell adhesion between trials.....	30
3.3 Microfluidic pump impact on glioma cell adhesion between different adhesion modification methods	40
4. DISCUSSION	44
5. CONCLUSIONS.....	49
SUMMARY	50
SANTRAUKA	51
ACKNOWLEDGMENTS.....	52
LITERATURE LIST.....	53
Suppl. 1.....	62
Suppl. 2.....	71

Abbreviations

BBB – blood-brain barrier

CAD – computer-aided design

COC – cyclic olefin copolymer

ECM – extracellular matrix

GBM – glioblastoma multiforme

IDH – isocitrate dehydrogenase

IPA – isopropyl alcohol

LOC – lab-on-a-Chip

PDMS – polydimethylsiloxane

SLA – stereolithography 3-D printing

TME – tumor microenvironment

INTRODUCTION

Gliomas are originated from altered progenitor cells that have aberrant brain development programs combined with unchecked local proliferation and diffuse infiltration into the brain stroma. Along certain tissue features, such as white matter tracts made up of myelinated axons and astrocyte processes, glioma cells invade, generating topologically complex cellular networks filled with hydrated, soft extracellular matrix (ECM) (Gritsenko and Friedl, 2018). Malignant gliomas are the most common type of primary brain tumor and with a variety of experimental therapies failing to show effectiveness in clinical trials it remains a challenging tumor to treat. The pathophysiological processes of angiogenesis and tumor cell invasion play key roles in glioma development and growth from the earliest stages (Shimizu et al., 2016). The glioma exhibits substantial infiltration of neoplastic cells, necessitating a profound comprehension of the molecular mechanisms governing tumor invasion to enhance therapeutic interventions. Cell surface receptors emerge as pivotal regulators of cellular adhesion and migration, playing essential roles in modulating crucial intracellular signaling pathways and serving as critical determinants at the interface between the cell surface and its microenvironment (D'Abaco and Kaye, 2007).

Various techniques for measuring cell adhesion have been extensively utilized across multiple disciplines, including biomaterial studies, tissue engineering, pharmacology, and cancer research. These methodologies aim to elucidate cell signaling pathways, assess the effects of biochemical treatments and environmental stimuli, and investigate the adhesion properties of normal and cancerous cells, among other applications (Khalili and Ahmad, 2015). Nevertheless, despite the precision offered by existing techniques, inherent limitations including low throughput, high equipment costs, time consumption, dependence on skilled operators, and variability in data due to operator factors are inevitable. These constraints highlight the imperative for the development of straightforward methodologies that circumvent the need for costly equipment, enabling the assessment of alterations in cell adhesion properties linked to diseases or specific physiological disruptions (Khalili and Ahmad, 2015).

Microfluidic chips present promising avenues for studying glioma cell adhesion in neuroscience research. However, the fabrication of microfluidic chips designed specifically for investigating glioma cell adhesion remains limited. Therefore, the development of an optimized microfluidic chip holds significant potential to advance our understanding of glioma pathogenesis and pave the way for novel therapeutic interventions.

Aim – to develop and optimize a microfluidic chip model for investigating glioma cell adhesion using various gelatin and collagen substrates. The objective is to elucidate the impact of substrate properties

on glioma cell behavior. By analyzing how these substrates affect glioma cell adhesion and migration, the study aims to enhance the understanding of the mechanisms underlying glioma invasion, ultimately contributing to the development of more effective therapeutic strategies.

Research tasks:

1. Optimized fabrication and characterization of a two – channel microfluidic chip separated with a porous polycarbonate membrane to simulate cellular interactions and fluid dynamics within a controlled environment.
2. Adapt coating protocols for gelatin and collagen solutions and establish adhesion testing methodologies.
3. Investigate glioma cell adhesion on the microfluidic chip under static conditions and with a microfluidic pump to simulate physiological conditions.
4. Perform microscopy to evaluate cell adhesion behavior in microenvironments and analyze the resulting data.

1. LITERATURE REVIEW

1.1 Glioma biology and cell adhesion mechanisms

Gliomas are the most common type of primary brain tumor, which can arise anywhere within the central nervous system (CNS), and are often fast growing with a poor prognosis for the patient. Gliomas are characterized by unregulated growth, apoptosis-resistance, diffuse invasion, strongly increased angiogenesis, and immunosuppression. Their complex cellular composition, diffuse invasiveness and capacity to escape therapies has challenged researchers for decades and hampered progress towards an effective treatment (Sedo and Mentlein, 2014). Gliomas are named according to the normal stromal (glial) cells of the brain they resemble most closely, such as astrocytes (astrocytomas), oligodendrocytes (oligodendrogliomas), and ependymal cells (ependymomas) (Fig. 1.1).

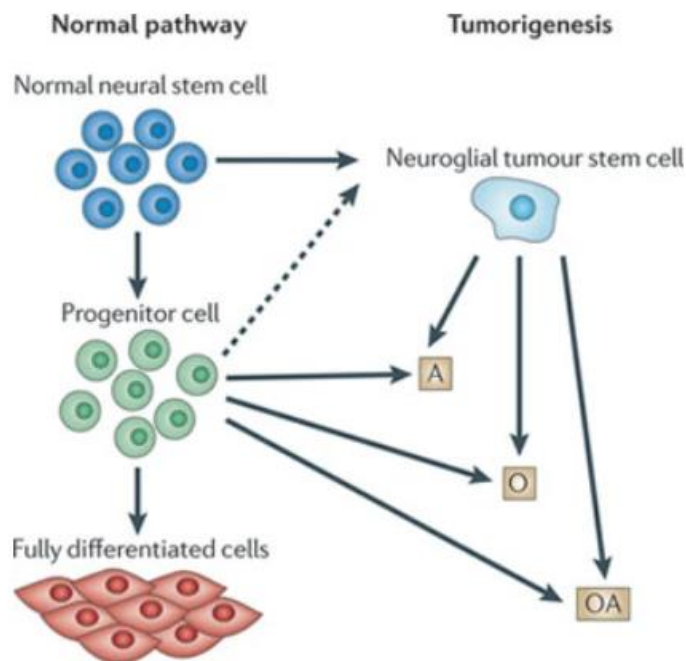


Fig. 1.1 Stem cell differentiation and tumorigenesis. All tumor types have the potential to originate from either multipotent stem cells or lineage-committed progenitor cells, as indicated by the arrows. Alternatively, there may be an initial formation of a tumor stem cell, represented by the dotted arrow, which then – depending on its lineage background – gives rise to different types of glial tumors, such as astrocytoma (A), oligodendroglioma (O), or a tumor that is a mix of these two types (OA) (Westphal and Lamszus, 2011).

In contrast to non-central nervous system (CNS) tumors, they exhibit diffuse infiltration throughout the brain, their originating organ, extending well beyond the visible tumor mass detected

by neuroimaging. While they typically remain confined within the CNS, reports of systemic dissemination remain rare (Westphal and Lamszus, 2011). Addressing this challenge requires innovative therapeutic approaches capable of targeting infiltrative tumor cells while minimizing damage to healthy brain tissue. When a suspected brain tumor is identified through imaging, referral to a specialized neuro-oncology team is essential for confirmation of diagnosis and subsequent management. For suspected glioblastoma, maximal surgical resection is typically the first-line approach to achieve local tumor control. Challenges in treatment arise in cases of elderly patients, those with poor performance status, or tumors unsuitable for surgical resection, where less invasive biopsy procedures or palliative measures may be considered due to high biopsy risk or unfavorable prognosis. Balancing therapeutic efficacy with patient-specific factors remains a critical challenge in glioma management (McKinnon et al., 2021).

The tumor microenvironment (TME) plays a crucial role in glioma behavior, influenced by interactions with the extracellular matrix, immune cells, and signaling molecules. Gliomas are mainly divided into isocitrate dehydrogenase (IDH) mutant and IDH wild-type (wt) tumors. In IDH-mutated gliomas, such interactions modulate tumor growth, progression, and clinical outcomes (Miller et al., 2021). Various studies reveal distinct immune signatures and macrophage involvement, impacting angiogenesis and tumor development. In contrast, IDH-wt gliomas exhibit unique TME characteristics, with potential implications for targeted therapies, such as immune checkpoint inhibitors and vaccines. Understanding these interactions holds promise for developing novel treatment strategies tailored to specific glioma subtypes (Di Nunno et al., 2022).

Gliomas are highly invasive tumors, and understanding how adhesion molecules facilitate their invasion into surrounding brain tissue is essential. Adhesion molecules mediate the interaction between glioma cells and the extracellular matrix (ECM), allowing them to migrate away from the primary tumor site and infiltrate healthy brain tissue. This process is a hallmark of glioma progression and contributes to the difficulty in treating these tumors effectively (Li et al., 2021). Adhesion molecules can confer resistance to various treatments, including chemotherapy and radiation therapy. By anchoring glioma cells to the ECM, these molecules can promote cell survival and protect against the cytotoxic effects of therapeutic agents. Understanding the mechanisms underlying this resistance can lead to the development of strategies to overcome it, improving treatment outcomes for patients with glioma (Jiang et al., 2019).

1.2 Microfluidic technology in a neuronal cell research

Microfluidics encompasses a versatile technology enabling precise manipulation of fluid behavior at microscale dimensions. Its applications span diverse disciplines including fluid dynamics, synthetic

and analytical chemistry, as well as biology and medicine. In these domains, microfluidics proves invaluable for evaluating drug toxicity, investigating drug delivery systems, advancing regenerative medicine, and conducting single-cell analyses. Its efficacy lies not only in facilitating meticulous control over fluid dynamics but also in uncovering and harnessing unique fluid properties absent in macroscopic systems (Saorin, Caligiuri, and Rizzolio, 2023). Additionally, the application of microfluidic technologies not only enables precise manipulation of fluid behavior at microscale dimensions but also presents significant advantages across various biotechnological applications. The wide ranging discipline of biotechnology covers a tremendous amount of technological ground — from the use of cells for production of pharmaceutical compounds and food aromas, to the development of assays for detection of disease, and even extending to the use of purified enzymes in various industrial applications (Fig. 1.2) (Enders, Grünberger, and Bahnemann, 2024).

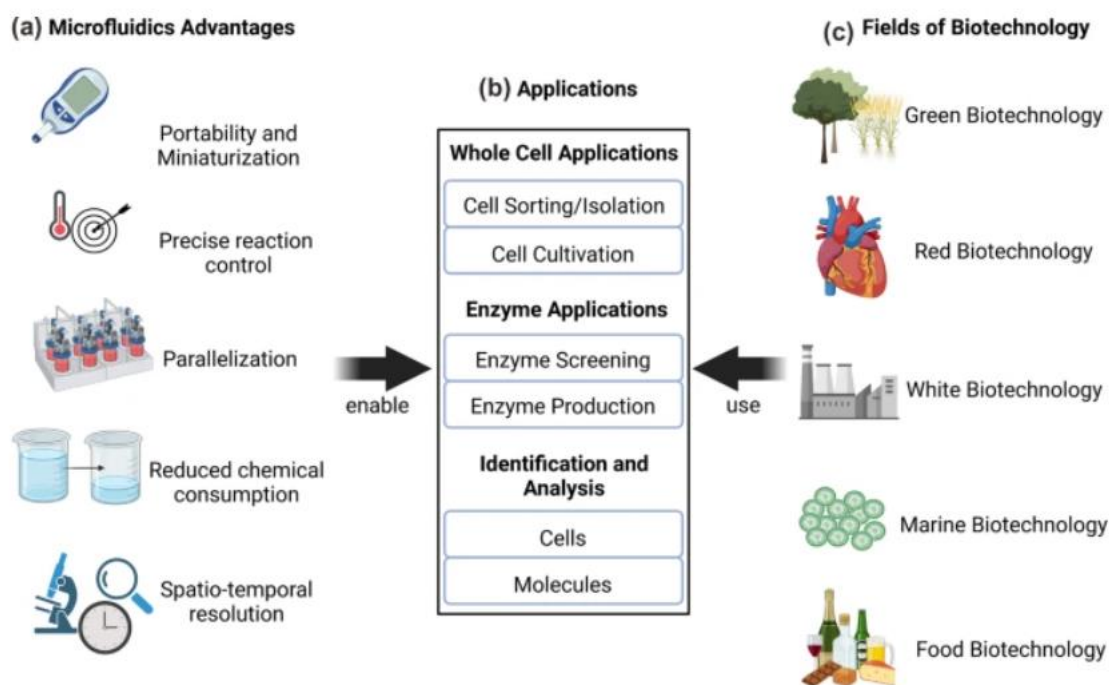


Fig. 1.2 Microfluidics advantages in applications of various fields of biotechnology. “Color” – based categorization approach clarify industrial applications: “red” biotechnology involves pharmaceutical and health applications; “yellow” biotechnology covers food science applications; “green” biotechnology encompasses agricultural uses; “blue” biotechnology revolves around marine and fresh water applications; and “white” biotechnology is reserved for those use cases which are purely industrial in nature (Enders, Grünberger, and Bahnemann, 2024).

Microfluidic chips are commonly used to precisely control fluids using channels that range in size from tens to hundreds of microns and is known as a “lab-on-a-chip”. The microchannel is small, but has a large surface area and high mass transfer, favoring its use in microfluidic technology applications including low reagent usage, controllable volumes, fast mixing speeds, rapid responses,

and precision control of physical and chemical properties (Whitesides, 2006). Microfluidics integrate sample preparation, reactions, separation, detection, and basic operating units such as cell culture, sorting and cell lysis and can mimic the environment of a physiological organ, with the ability to regulate key parameters including concentration gradients, shear force, cell patterning, tissue-boundaries, and tissue–organ interactions. The major goal of microfluidics is to simulate the physiological environment of human organs (Wu et al., 2020).

To trigger the spread of cancer to distant sites via the bloodstream, tumor cells encounter diverse physical challenges within microenvironments. They must navigate through the stroma, penetrate the endothelial barriers to enter blood or lymphatic vessels, travel through the vessels, exit into surrounding tissues, and establish new colonies at secondary sites (Chambers, Groom, and MacDonald, 2002). In soft tissues, cancer cells are exposed to mechanical forces such as fluid shear stress, exerted on circulating tumor cells by blood flow in the vascular microenvironment, and also on tumor cells exposed to slow interstitial flows in the tumor microenvironment (Mitchell and King, 2013). Shear stress, induced by liquid flow, is known to actively participate in proliferation, apoptosis, invasion, and metastasis of tumor cells and exerted on the tumor cell surface were estimated to be quite low (less than 0.05 dyn cm^{-2}). Such shear stresses and rates can affect cancer cell viability and thus the chances of metastasis (Huang et al., 2018). Shear stress mimics the mechanical forces present in physiological environments such as blood vessels and lymphatic channels. Cancer cells often metastasize via these routes, and understanding how they respond to shear stress can provide insights into their migratory and invasive capabilities (Qazi, Shi, and Tarbell, 2011).

Furthermore, this microfluidic technology enable new insights into neurobiological events previously unachievable through traditional cell biology techniques. Several neural system models, including animal models, 2-D and 3-D cell cultures, and clinical studies, are utilized to explore the CNS's physiological and pathological functions in neuronal diseases. However, each model presents challenges (Neto et al., 2016). While animal models are crucial, they may not accurately represent human neural systems due to differences in brain structure and cognitive functions. Clinical trials have also shown discrepancies from promising pre-clinical results in animal models. Classical 2-D cell cultures have limitations in assessing drug responses in complex diseases and fail to mimic tissue architecture accurately. Three-dimensional models, like organoids, offer promise in recapitulating organ function but face challenges in structural variability and predicting cell positions accurately for assessing neural network activities (Mofazzal Jahromi et al., 2019). Thus is why microfluidic systems can create a powerful micro engineered scaffold-free or scaffold-based tool for the manipulation, monitoring, and assessment of neuronal cells, and for use in drug discovery with high specificity and resolution (Babaliari, Ranella, and Stratakis, 2023). The microfluidic "organ-on-a-chip" technology

offers a cost-effective and rapid approach for manipulating, monitoring, and evaluating cells, aiding in drug discovery. These chips enable cell culture in minute fluid volumes, overcoming limitations of 2-D and 3-D cultures and animal models. Stem cells, including neural stem cells, induced pluripotent stem cells, and embryonic stem cells, can generate various neural cells. Thus, combining microfluidic organ-on-a-chip with stem cells presents a promising avenue for studying treatments for central nervous system (CNS) and peripheral nervous system (PNS) disorders and diseases (Mofazzal Jahromi et al. 2019).

1.3 Microfluidic chip models of the blood-brain-barrier for glioma research

Microfluidics offers useful experimental tools for studying cellular neuroscience, which involves imitation of neural structures within a microscale device (N. Lee et al., 2014). Compared with conventional culture systems, a microfluidic device can provide a physiologically more relevant cellular environment, by generating fluid flows which can maintain a more constant and soluble microenvironment (Breslauer, Lee, and Lee, 2006).

Recently, this microfluidic technology has been developed to study organ-on-chip models of the blood-brain barrier (BBBs-on-chips) (van der Helm et al., 2016). The BBB is a diffusion barrier that prevents most substances from entering the brain from the blood. The BBB is made up of three biological parts of the brain microvasculature: endothelial cells, astrocyte end-feet, and pericytes (Fig. 1.3). Tight junctions between cerebral endothelial cells constitute a diffusion barrier, preventing most blood-borne chemicals from entering the brain. Astrocytic end-feet tightly ensheath the vessel wall and appear to be crucial for tight junctions barrier induction and maintenance. BBB protects the brain from harmful compounds from the blood and provides homeostasis for optimal neuronal function. BBB dysfunction, such as disruption of the tight junctions seal, affects a variety of neurologic illnesses, including stroke and neuroinflammatory disorders (Ballabh, Braun, and Nedergaard, 2004).

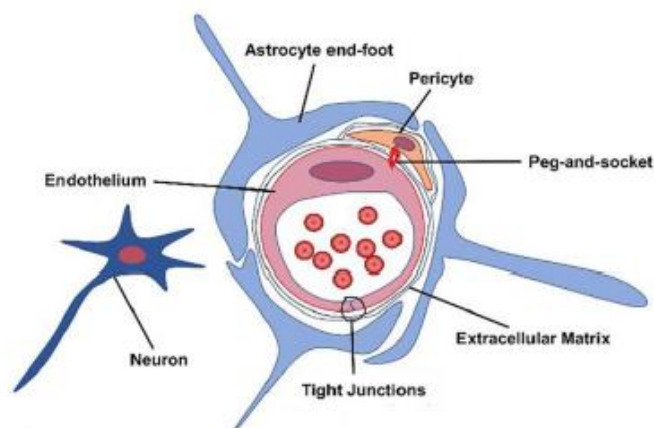


Fig. 1.3 The blood-brain barrier (BBB) is composed of specialized endothelial cells, pericytes, extracellular matrix, glial cells, and neurons (Xiao et al., 2020).

Although the BBB represents an essential barricade for the purpose of brain protection, it also serves as a barrier to therapeutic interventions during brain tumor progression, and because of this a number of chemotherapeutic drugs such as vincristine, paclitaxel, etc., are unable to reach the brain (Pardridge, 2005). Therefore, effective in vitro BBB models are essential to study the neurovascular unit's microenvironment and understand BBB behavior, which is crucial for designing brain tumor treatments. While animal models have provided valuable insights, they do not fully translate to human conditions and their complex physiology makes real-time cellular studies challenging. To achieve successful clinical translation of therapies, it is crucial to develop an in vitro model that accurately mimics the BBB's anatomical, physiological, structural, and functional aspects, including interactions with therapeutic molecules, in real time (Esch, Bahinski, and Huh, 2015).

To overcome these limitations, microfluidic-based 3-D in vitro BBB models have gained significant attention for their ability to accurately replicate the physiological aspects of the BBB (Hajal et al., 2018). Microfluidic platforms have evolved from the traditional Transwell design, which uses porous membranes between upper and lower channels to create a sandwich-like assembly. These platforms model the blood-brain barrier (BBB) with separate neural and vascular channels divided by a membrane. Typically, endothelial cells (ECs) are cultured in the upper channel, while the lower channel is used for other brain cells such as pericytes and astrocytes. The dual-channel system facilitates the flow of culture medium, mimicking the dynamic nature of circulating blood and the ECM (Walter et al., 2016). The porous polycarbonate membrane is essential for modeling the selective permeability of the BBB. These pores allow for the exchange of nutrients, waste products, and signaling molecules between the upper and lower channels, simulating the natural interactions that occur in the BBB. This setup enables researchers to study the permeability of the BBB and the transport mechanisms of various therapeutic agents in real time. By adjusting the size and density of the pores, the microfluidic device can closely mimic the selective permeability of the BBB, providing a reliable platform for testing the efficacy and safety of new drugs. This level of control and precision is essential for developing effective therapies that can bypass the BBB and target brain tumors directly (Sood et al., 2022).

1.3.1 Materials used for construction of microfluidic chip for glioma cell research

A microfluidic device can be constructed from a wide variety of materials. Each one of these materials has distinct characteristics and, as a result, behaves differently throughout processing (Kenari et al., 2022.). Currently, microfluidic materials are categorized into three main groups: inorganic, polymers, and paper: 1) inorganic materials include silicon, glass, co-fired ceramics, and vitroceraamics, 2) polymer-based materials are divided into thermoset and thermoplastic subcategories. Thermoset materials are cured using heat or UV light, while thermoplastics are

thermoformable for rapid prototyping. Both types offer a range of mechanical properties from rigid to elastomeric, and their surface properties can be extensively modified through chemical adaptations (Roy et al., 2016). Fabrication with polymers is easy, and their use as materials reduces the time, complexity, and cost of prototyping and manufacturing. In general, microfluidic systems are made by molding and bonding replicas in elastomers such as polydimethylsiloxane (PDMS), or thermoplastics like polymethyl methacrylate (PMMA) or polycarbonate (PC). Other materials, such as cyclic olefin copolymer (COC) and SU-8, are increasingly valued in the field of microfluidics. These polymers are favored due to their essential properties: biocompatibility, optical transparency, cost-effectiveness, and lack of intellectual property restrictions (Marquet, 2023). Hence, manufacturing techniques must be tailored to the specifics of the material and its limitations. In addition to the manufacturing method cost, it is crucial to choose an appropriate manufacturing method for microfluidic systems (Kenari et al., 2022.)

1.3.1.1 Mold modeling and 3D printing

Stereolithography 3-D printing (SLA) is commonly known as resin 3-D printing. SLA 3-D printers use light-reactive thermoset materials called “resin”, which is uncured liquid plastic. When SLA resins are exposed to certain wavelengths of light, short molecular chains join together, polymerizing monomers and oligomers into solidified rigid or flexible geometries (hardened plastic). SLA parts have the highest resolution and accuracy, the sharpest details, and the smoothest surface finishes of all current 3-D printing technologies (Waheed et al., 2016). Hence, the ability to fabricate a complete microfluidic device in a single step from a computer model is very advantageous (Bhattacharjee et al., 2016).

3-D printing is advantageous for prototyping and replication of products, thus is why it is used to fabricate a master mold that may be used for soft lithography using polymers such as polydimethylsiloxane (PDMS) (Kamei et al., 2015). Fabricating PDMS-based microfluidics using 3-D printed master molds provides many of the advantages of 3-D printing fabrication and maintains the desirable PDMS material properties such as biocompatibility and oxygen permeability. The master may be produced via rapid prototyping techniques, reducing the overall cost and time required for fabrication, followed by traditional PDMS molding, and the convenience of these fabricated PDMS templates can be seen in that they do not require a cleanroom (Amin et al., 2016). Also, the use of 3D-printed molds for PDMS devices is particularly promising for cell culture applications. Gross et al performed a study with 3-D printed microfluidic electrical cell lysis devices that has been coated with PDMS, and the results showed improved cellular adherence for cell lysis (Gross et al., 2015). Another study was done with 3-D printed soft lithography mold for examining concentration

gradients for biomedical applications. The mold was fabricated by an ink-jet 3-D printer and cured using UV light and PDMS was poured into the mold to create a 5 mm thick lab-on-chip device. This device was then used to examine the effect of concentration gradients of growth factors and the effect of embryonic stem cell survival and growth (Kamei et al., 2015). Therefore, 3-D printing shows promise to add broad and novel applicability to several research domains.

1.3.1.2 Polydimethylsiloxane

In replication of microfluidic master structures for molding or soft embossing by double casting of microstructured masters in fabrication of microchips, PDMS mold is usually used (Gitlin, Schulze, and Belder, 2009). PDMS molds provides a reliable, simple and cost-effective way to construct microstructures in materials. As to the structures with shallow features in large intervals, PDMS replica can attain high precision (Ye et al., 2009). Another key aspect pertinent to microfluidics is the transparency, which enables the direct optical access into microchannels for real-time monitoring of the process. Further, PDMS is found to show excellent biocompatibility and permeability and low autofluorescence, opening a wide arena in the field of biotechnology and biomedical engineering (Raj M and Chakraborty, 2020).

PDMS microchips can be fabricated through microscale molding processes, where a silicon wafer with patterned photoresist can be used as a mold master. After the patterning, prepolymer of PDMS is poured into the mold master. And then cured PDMS is peeled off from the master to be pasted on a flat plate (Fig. 1.4) (Fujii, 2002).

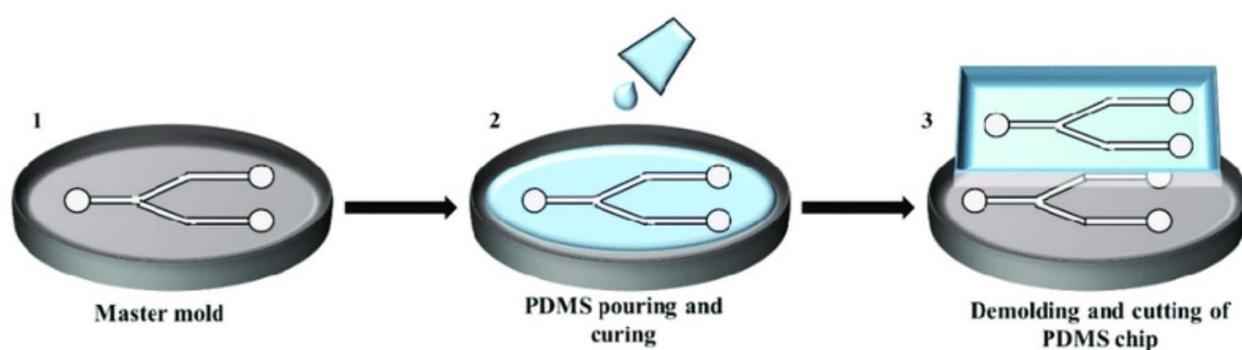


Fig. 1.4 Fabrication process of a PDMS chip molding: 1) Generating silicon master mold using photolithography. 2) Pouring the mixture of PDMS prepolymer and curing agent into the master mold. 3) Peeling of the solidified PDMS from the master mold (Akther et al., 2020).

Fig. 1.4 presents a PDMS microchip which has microchannels for electrophoretic separation that can be easily fabricated through a molding process. Therefore, PDMS-based microfluidic devices enable

us to realize microchips for biomedical applications in a relatively easy and cost effective way (Fujii, 2002).

However, apart from these qualities, one challenge with the PDMS is that they seldom facilitate cell adhesion or attachment. It is known that in cell-biomaterial studies, cell attachment is the initial step. It plays a crucial role in the cellular processes such as cell proliferation and cell differentiation. In Lab-on-a-Chip (LOC) applications the absorption of molecules onto PDMS surface aggravates in presence of a favorable pH. It also tends to swell in many common solvents, especially hydrocarbon-based ones. Another issue is the inherent hydrophobicity of PDMS which may be resolved with a plasma exposure, but not to last for a long time. This is a serious issue in biological assays as it enhances the protein absorption. Other downsides include evaporation of water through PDMS (Raj M and Chakraborty, 2020). To overcome these challenges, microfluidic channels could be coated with a cell-compatible hydrogel layer inside a PDMS-layered device (Leclerc, Sakai, and Fujii, 2003; Rosser et al., 2015). Coating PDMS with a hydrogel anchored by micropillars is a creative approach to generate a more stable and effective hydrophilic surface, as PDMS virtually does not swell in contact with water. Thus, PDMS and hydrogel act as a perfect combination, because hydrogel contains water providing a very hydrophilic surface with remarkable biocompatibility and similarity to biological tissues, and PDMS serves as a more rigid substrate for the soft hydrogel film (Xu et al., 2021).

1.3.1.3 Cyclic olefin copolymer

Cyclic olefin copolymer (COC), a new amorphous engineering thermoplastic, recently has gained a lot of attention in usage for many kinds of optical, electrical, and mechanical applications due to its outstanding properties of higher transparent, lower birefringence, lower dispersion, and lower water absorption (Wang et al., 2007). COC is a comparatively new thermoplastic material and has been gaining popularity in LOC fabrication due to its better chemical properties, such as high chemical resistance and good optical transparency in the near UV range and ease of fabrication (Nunes et al., 2010). Through its characteristic molecular structure and superior catalyst technology, COC offers a wide range of grade variations, in terms of flow properties and heat resistance and as a result an appropriate substrate material for the microdevice (Jena, Yue, and Lam, 2012).

Although COC based microfluidic devices have been widely used, some limitations exist. Devices made up of COC are not optimal for studies involving pharmaceuticals because of its hydrophobic surface, which makes it prone to spontaneous nonspecific protein adsorption and cell adhesion when exposed to biological tissues or fluids. In order to minimize adsorption of analytes such as proteins and to reduce the adhesion of cells, it is necessary to chemically and physically modify the COC

surfaces (R. K. Jena and Yue, 2012). Numerous modification processes can be used to modify the plastics surface – flame treatment, UV/ozone treatment, corona discharge treatment, and various types of plasma treatment (Hwang et al., 2008). In plasma treatment of polymers, the main factors thought to be responsible for the effects on the surface are – free radicals present in the plasma, vacuum UV radiation in the chamber, and impingement of ions on the surface. With plasmas derived from simple gases (oxygen, nitrogen, noble gases, etc.) the major modification effect can be described as – ablation or etching, degradation of polymer molecules, cross linking or branching of near-surface molecules, and introduction of new function groups. The etching effect means the polymer surface was ion bombard by plasma. The degradation of polymer molecules of the sample surface is caused by the induced thermal energy during plasma treating. A simple way to modify the chemical and physical states of the material surface is done by plasma treatment without altering the bulk properties. Also, there are no chemical solvents and poison gases to be used in modified process by plasma treatment, which also fits the green modification process (Johansson et al., 2002; Hwang et al., 2008). Therefore, to improve the surface adhesive ability of the COC substrate, oxygen plasma treatment is utilized.

1.3.1.4 Off-stoichiometry thiol–ene

Off-stoichiometry thiol–ene (OSTE) is a promising alternative material class to PDMS. Thiol-ene polymers have been used in microfabrication techniques due to its chemical resistance to different types of solvents, fast curing, low gas permeability, ability to seal against glass, tunable mechanical properties and lack of oxygen polymerization inhibition (de Campos et al., 2017). The use of UV curable off-stoichiometry thiol–enes offers multiple essential features due to the excess of thiol or epoxy groups during the curing stages. Excess of thiol groups on the surface allows for easy modification of the OSTE surfaces either after UV polymerization or after thermal curing steps via the thiol and hydroxy chemistries, respectively. After thermal polymerization, OSTE becomes hard and obtains its final material properties (Rimsa et al., 2021). As one of the advantages, the curing time can vary from 30 to 180 s, which is much faster than PDMS preparation, and it is possible to bond two flat pieces of OSTE cured polymers through click reaction. This method can be used to bond multiple layers of substrates, and different structures can be incorporated to the device, such as silicon photonic sensors. The presence of readily available functional groups on the surface of OSTE substrates also allows the anchoring of different substances, such as proteins, without the need of previous surface treatment or modification (Saharil et al., 2012; Errando-Herranz et al., 2013).

Therefore, OSTE thermosets show low permeability to gases and little absorption of dissolved molecules, allow direct low-temperature dry bonding without surface treatments, have a low Young's

modulus (ratio of strain to stress), and can be manufactured via UV polymerization. For these reasons, OSTE have recently gained attention for the rapid prototyping of microfluidic chips (Borda et al., 2023).

1.3.1.5 Polycarbonate membrane

Membranes are defined as a porous or dense barrier that permit the passage of certain compounds selectively in a fluid. The permeation of molecules through a membrane barrier is driven by a variety of forces such as concentration gradient, pressure difference, thermal variation, electrical force and so on (Jong, Lammertink, and Wessling, 2006). Membrane technology exhibits many inherent advantages including cost-effective, operation-convenient, function-versatile and environment-compatible compared with conventional separation techniques. Thus is why combining membranes with microfluidics can magnify their respective advantages to provide more valuable applications (Chen and Shen, 2017).

In order to create membranes with controllable transport properties, the ability of the macromolecules at the surface layer to make reversible conformational transitions is used. The research in this direction is related to a goal-directed formation of a membrane surface with tailored chemical structure. For this purpose, membranes are modified by deposition on the surface of thin polymeric layers obtained by plasma polymerization (Çökeliler, 2013). The usage of plasma provides additional advantages such as – the control of the thickness of the polymeric layer deposited on the membrane surface, the high adhesion of the layer, the short treatment time, and the opportunity of using of a wide list of organic and element-organic compounds for modification (Kessler et al., 2003).

Nowadays, membrane technology has been widely used in chemical industry and biological engineering (Chen et al., 2016). Lee et al. presented a microfluidic device for the detection of gaseous odorants which more closely mimics the human olfactory system (Lee, Oh, and Park, 2015). To et al. proposed a microdialysis system integrating microfluidic channels and nanoporous filtering membranes, aiming at a fully implantable system that drastically improves the quality of life of patients (To et al., 2015). Various studies have also described polycarbonate membrane applications in drug screening. Kuhn et al. presented a versatile method to study the kinetics of tetracycline permeation across liposome membranes on a microchip (Kuhn et al., 2011). Therefore, membranes in microfluidics have been used in many chemical and biological fields.

1.4 Microfluidic chip surface adhesion modification methods

Cell adhesion is fundamental for anchorage-dependent cells to thrive on the matrix, initiating a cascade of cellular processes including diffusion, migration, proliferation, and differentiation. This

adhesion is critical in various biological processes such as cancer metastasis and wound healing. In vivo, cells are enveloped by the extracellular matrix (ECM), whose physical and biochemical characteristics can influence cell function and behavior, triggering cellular responses. Moreover, cell adhesion serves as the foundation for cell communication with the external environment and is crucial for tissue development (Cai et al., 2020). Cells adhere to specific surfaces through integrins, which are a family of cell surface receptors that mediate the attachment between a cell and its surrounding environment. Without proper adhesion, cells often undergo apoptosis. Therefore, engineering an appropriate culture substrate to direct cellular behavior and function is a critical issue in the fields of regenerative medicine and tissue engineering.

Collagen coating is a common surface adhesion enhancement treatment. Collagen, an abundant structural protein in animals, is a major component of the ECM, making up one-third of total protein in humans and three-quarters of the dry weight of skin (Shoulders and Raines, 2009). Experiments by Zhao et al. demonstrated that C2C12 cells had a higher proliferation rate on collagen-treated substrates compared to untreated samples. Additionally, cells grown on foldable microplates modified with collagen showed better adhesion strength, conducive to microplate folding (Zhao et al., 2021).

Gelatin, a partially degraded derivative of collagen, is another natural polymer widely used to enhance material biocompatibility and facilitate cell adhesion, migration, proliferation, and differentiation (Wu et al., 2023). Gelatin retains numerous RGD (Arg-Gly-Asp) motifs, which are recognized by cell surface integrins to enhance adhesion (Haug and Draget, 2009). Studies by Zhang et al. on polyvinyl alcohol/gelatin hydrogels revealed that higher gelatin concentrations increased protein adsorption capability and improved cell adhesion area and morphology (Zhang et al., 2022). This suggests that gelatin solutions could effectively enhance cell adhesion on microfluidic chip surfaces.

In conclusion, surface modifications using collagen and gelatin provide enhanced adhesion properties necessary for the successful cultivation of cells.

2. METHODOLOGY

2.1 Design and fabrication of the microfluidic chip

In this section, the comprehensive design and fabrication process of the microfluidic chip is presented. Due to the complexity of the two-channel configuration separated by a porous membrane to simulate cellular interactions, the chip underwent a meticulous series of steps to ensure precise functionality and reliability. From initial conceptualization to final fabrication, each stage was carefully executed to achieve optimal performance. The following subsections detail the various methodologies employed, including computer-aided design (CAD) design, photolithography, etching, and bonding processes. Through this detailed exploration, the intricate steps involved in realizing the microfluidic chip's design and structure are elucidated (for a comprehensive protocol see Suppl. 1).

2.1.1 Mold modeling and 3D printing

Master molds bearing pseudo positive design of LOC were designed in CAD modeling software “Autodesk Fusion 360”. Molds for PDMS were 3-D printed with Anycubic Photon stereolithography 3-D printer from medical grade light sensitive resin. Using “Autodesk Fusion 360” software, model of microchip was designed and exported in a 3-D printable file format (STL or OBJ). Each lithography based printer includes software to specify printing setting and slice the digital model into layers for printing (Fig. 2.1). Once setup was complete, the printing begins.

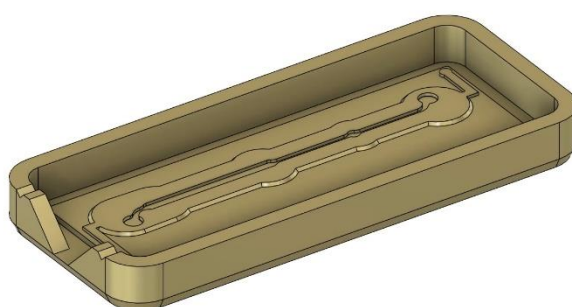


Fig. 2.1 Master mold of LOC designed in CAD modeling software “Autodesk Fusion 360”.

After the printing process begins, the machine can run unattended until the print is completed (Fig. 2.2).



Fig. 2.2 Completed 3-D printed master molds for lab-on-a-Chip fabrication. Bottom and top parts shown on the left and right sides, respectively (Photo courtesy of the author).

Once the printing was completed, printed mold required rinsing it in isopropyl alcohol (IPA) to remove any uncured resin from their surface. After rinsing, some materials required post-curing, a process which helps parts to reach their highest possible strength and stability. In our case post-processing included mold washing in IPA in ultrasonic bath twice for 3 min and UV curing for 30 min.

2.1.2 PDMS casting

All the masters (Fig 2.3) for each layer were fabricated by Anycubic Mono X6KS stereolithography 3-D printer. The fabrication processing steps are described as follows:

1. A piece of PDMS layer was produced with silicone elastomer mixture (SYLGARD™ 184 Silicone Elastomer) at a weight ratio of base : curing agent = 10 : 1.
2. Mixed silicone elastomer and curing agent then placed in a vacuum chamber to get rid of the bubbles.
3. Vacuumed silicone elastomer is poured into a “pseudo positive“ silicone mold, 3-D printed form, that has patterned relief structures on its surface.
4. Silicone mold with silicone elastomer was then cured for 24 h in 60 °C temperature.
5. Then hardened “negative” PDMS shape with specially designed grooves was taken out of the form.



Fig. 2.3 PDMS masters. Bottom and top parts shown on the right and left sides, respectively (Photo courtesy of the author).

In our methodology we work with PDMS, on the basis of its easy molding characteristics, transparency, for more effective UV curing of other materials e.g COC, and flexibility. Moreover, it had already been used in the transferring layer of designed grooves, specifically in the fabrication of 3-D structured photocurable polymers.

2.1.3 Preparation of COC

The substrate (COC) (Fig. 2.4.) was prepared in advance following:

1. Ultrasonic cleaning, which is a process that uses ultrasound (usually from 20 to 40 kHz) to agitate a fluid, with a cleaning effect. First cleaning of the COC was done with acetone, second with IPA.
2. Then oxygen plasma treatment was done to COC. Oxygen plasma refers to any plasma treatment performed while introducing oxygen to the plasma chamber. Oxygen was used to clean surfaces prior to bonding.

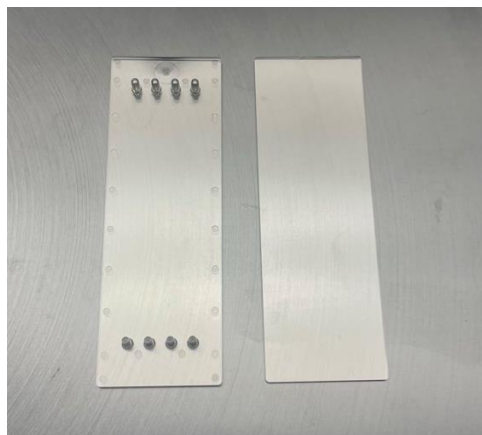


Fig. 2.4 The substrates of COC. Bottom and top parts shown on the right and left sides, respectively (Photo courtesy of the author).

2.1.4 OSTE injection casting

The fabrication process is schematically demonstrated in Fig. 2.5. The fabrication processing steps are described as follows:

1. COC was placed within the PDMS mold.
2. PDMS mold containing COC was inserted into a casing, through which uncured OSTE was injected onto the COC.
3. A specific UV light exposure time was set by the „Arduino IDE“ software installed on the computer.
4. Once OSTE was injected, the casing containing PDMS, COC, and uncured OSTE was exposed to UV light for 15.5 seconds.
5. Following the 15.5 second exposure, COC substrate with hardened OSTE were carefully separated from the PDMS mold.

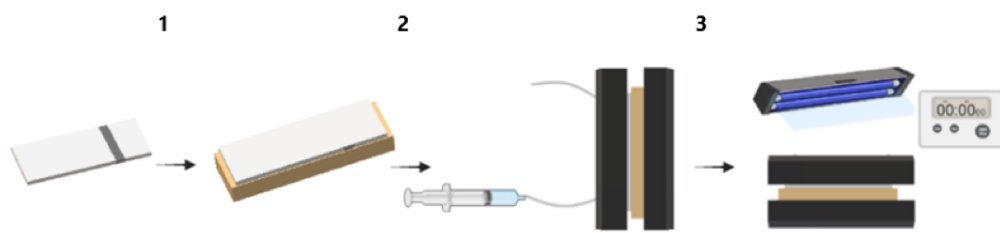


Fig. 2.5 Schematical demonstration of OSTE injection : 1) COC was placed in PDMS. 2) PDMS with COC were placed in a casing, through which uncured OSTE was injected. 3) Curing with UV light.

2.1.5 Polycarbonate membrane preparation and placement

1. A 3 μm porous polycarbonate membrane was cut in width and length to match the dimensions of the microchip channel. The 3 μm pore size was selected based on its suitability for mimicking the size restrictions and permeability characteristics of the blood-brain barrier (BBB)
2. Before polycarbonate was positioned onto COC with hardened OSTE, it underwent activation via oxygen plasma treatment.
3. After oxygen plasma treatment polycarbonate membrane was placed onto COC with hardened OSTE.

2.1.6 Construction of microfluidic chip

1. Another set of PDMS and COC substrates, with different patterned relief structures on their surface, were fabricated following previous steps (2.1.1 – 2.1.4).

2. Subsequently, the COC substrate with the polycarbonate membrane and the COC substrate without the membrane were assembled together to form the microfluidic chip (Fig 2.6).
3. The assembled microfluidic chip was cured at 60 °C temperature for a duration of 24 hours.

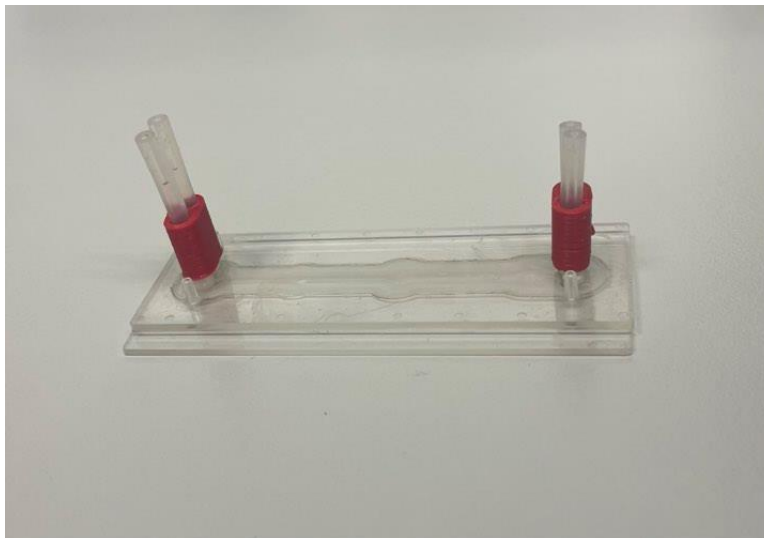


Fig 2.6 In house made microfluidic chip (Photo courtesy of the author).

It is important to note that various microfluidic fabrication processes were performed in a clean room. Other potential contaminants, including as chemical vapors and specific light wavelengths, were also kept away from the microfabrication process in a clean room.

2.2 Cell line and culture conditions

C6 cells, a rat glioma cell line, were utilized in this experiment. These cells are commonly used in cancer research due to their rapid proliferation and well-characterized behavior. The C6 cell line was obtained from a cell bank, ensuring their quality for the study.

2.3 Preparation of microchip channel for glioma cell adhesion

The microchip channel was prepared for cell adhesion by coating the channel surface with three types of gelatin, collagen and a mixture of collagen and gelatin:

1. For channel coating three types of gelatin were used – gelatin 38, gelatin 175 and gelatin 300, the numbers refers to their bloom strength, which is a measure of the gel strength (Sigma-Aldrich).
2. 1 % gelatin 38, gelatin 175 and gelatin 300 solutions were made by mixing 0.3 g of chosen gelatin and 30ml of phosphate – buffered saline (PBS). The choice to use 1% gelatin solutions was based on several scientific and practical considerations related to the properties of the materials and their effects on cell adhesion – a 1 % gelatin solution provide a manageable viscosity for coating and filling microfluidic channels, while still maintaining enough structural integrity to support cell

adhesion. Once the gelatin was fully dissolved, the solutions were sterilized by filtration through a sterile filter membrane.

3. Similarly, 0.5 % collagen (Sigma-Aldrich) solution was made by mixing 0.15 g of collagen and 30 ml of PBS. A 0.5 % collagen solution was chosen for its ease of use and ability to form a stable gel that promotes cell attachment and proliferation. Once the collagen was fully dissolved, the solution was sterilized by filtration through a sterile filter membrane.
4. Mixture of collagen and gelatin was made by mixing already made 0.5 % collagen with 1 % gelatin 175 with ratio 1:1, respectively. The selection of gelatin 175 for mixing with collagen in the experiment was made as part of an exploratory approach to optimize cell adhesion substrates. Given the variety of gelatin types available, gelatin 175 was chosen to investigate its potential efficacy in combination with collagen.
5. The microchip channel was thoroughly cleaned and sterilized with 70 % ethanol and washed with distilled water.
6. Then each substrate solution was introduced into separate channels of the microchips and incubated in room temperature for 1 hour to allow proper substrate binding and surface coating.
7. After incubation, substrate solutions were removed and microchip channels were washed with PBS to remove any unbound substrate molecules.

2.4 Preparation of Glioma cell culture

Preparation of glioma cells involved several steps to ensure their proper growth and maintenance in culture:

1. Glioma cells were cultivated in a sterile, controlled laboratory environment. The first step involved thawing frozen glioma cells obtained from a cell bank. The cells were quickly moved to a sterile laminar flow hood after being swiftly thawed in a water bath at 37 °C.
2. After being defrosted, the glioma cells were seeded into tissue culture flasks that were filled with RPMI (Roswell Park Memorial Institute) medium, that has been enhanced with antibiotics (penicillin-streptomycin) and fetal bovine serum (FBS). RPMI medium was supplemented with essential nutrients, vitamins and amino acids to support growth and proliferation of glioma cells.
3. Following a gentle mixing step to guarantee even distribution, the cell suspension was incubated at 37 °C in a humidified environment containing 5 % CO₂. In order to evaluate the cells adhesion and proliferation, they were periodically monitored under a microscope.
4. The RPMI medium was changed every 2 – 3 days in order to provide fresh nutrients and remove waste products. When the cells achieved 80 % – 90 % confluence, they were passaged to prevent overgrowth and maintain optimal conditions for cell growth.

2.5 Cell attachment and seeding in microchip

After microchip channels were coated with adhesive substrate solutions and glioma cells have been cultured and grown to the desired confluence in tissue culture flasks, they were prepared for seeding into a microchip:

1. Glioma cells were detached from the tissue culture flask using trypsinization method. This process involves treating the cells with a trypsin enzyme solution to break down cell – cell and cell – substrate adhesions, allowing the cells to detach from the culture surface.
2. After detachment, the trypsin was neutralized by adding cell culture medium (RPMI), This prevents the trypsin from causing damage to the cells, and centrifuged.
3. Then glioma cells were resuspended in a 1 ml suitable cell culture medium (RPMI) to create a homogeneous cell suspension.
4. The detached and centrifuged glioma cells were then counted using hemocytometer to determine the cell concentration. This step ensured that the appropriate number of cells was seeded into the microchip to achieve the desired cell density.
5. Once the cell suspension was prepared, one million glioma cells were carefully injected into the microchip channel to ensure an equal number of cells in each channel.
6. After seeding, the microchip containing glioma cells was incubated at 37 °C in a humidified environment containing 5 % CO₂.
7. The seeded glioma cells were monitored periodically under a microscope to assess their adherence and growth within the microchip. Additional culture medium (RPMI) was changed every day for 6–7 days to maintain cell viability and growth.

2.6 Microfluidic chip monitoring using a microscope and image capturing

1. After 6–7 days of incubation, the seeded cells were monitored under a Nikon inverted fluorescence microscope „Eclipse Ti“ equipped with the „NIS-elements“ software. The „NIS-elements“ software allows for real-time observation of cell behavior, morphology, and adhesion. High-resolution images of the cells were captured using the „NIS-elements“ software and 20x lens, providing visual documentation of the cell culture process.
2. A comprehensive array of images capturing the entire microfluidic channel was obtained.
3. Collected images were processed using image analysis software „ImageJ“, a subset of five representative images was chosen for subsequent analysis to quantify both non-adherent and adherent cell populations (Fig. 2.7).

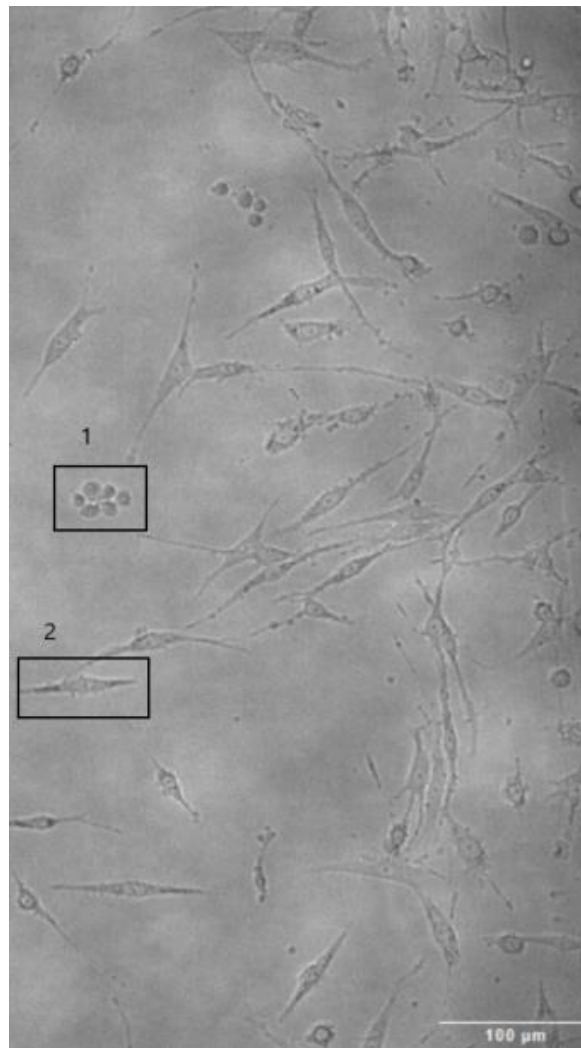


Fig. 2.7 Non-adherent and adherent cells photo example. Scale bar: 100 µm. 1 – non-adherent cells, 2 – adherent cells. (Photo courtesy of the author).

4. The number of cells per unit area were calculated for each image, providing a measure of cell density.

2.7 Microfluidic technique

1. Following the initial monitoring, the microchip was connected to a pump (Infusetek, model no.:ISPLab02) to initiate microfluidic flow within the channel.
2. PTFE (PolyTetraFluoroEthylene) tubing with 0.8 mm inner diameter and silicon tubing with 1 mm inner diameters (Darwin Microfluidics, Paris, France) were used for connections of the syringe pump and microchip.
3. The pump introduced a cell culture medium (RPMI) into the microchip channels, creating a controlled flow environment with 0.29 µl/min flow rate. Microfluidic calculator provided by Elveflow determined the flow rate within the microfluidic channel based on the dimensions (height – 1.2 cm, length – 5.8 cm, width – 0.2 cm) of the channel and the experimental parameters

(Fig. 2.8). In the design and optimization of microfluidic systems for studying cell adhesion, accurate determination of fluid flow parameters is crucial. Utilizing an online microfluidic calculator specific parameters were inputted: 1) the fluid properties were defined, selecting a RPMI medium with 10 % serum (FBS) to mimic physiological conditions; 2) negligible tubing resistance was assumed given the use of short, wide tubing commonly employed in microfluidic setups; 3) the channel geometry within the chip was accurately defined as a rectangular channel, with dimensions corresponding to the actual chip; 4) the selected shear stress value of 0.001 dyn/cm^2 was chosen to simulate conditions representative of the microenvironment surrounding tumor cells, where low fluidic stresses are often encountered. This adjustment aligns with recent literature suggesting that tumor cells experience minimal shear stresses in vivo, hence warranting the utilization of such low values in our calculations.

Part 1: Fluid properties

Describe the fluid **inside your reservoir**.
Chose predetermined fluid or custom **density**
and **viscosity**:

Medium with 10% Serum | ▾

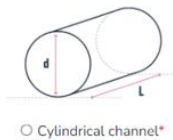
Density: **1000** Kg/m^3
Viscosity: **0.00072** Pa.s

Part 2: Tubing resistance (optional)

- Negligible tubing resistance
 High tubing resistance

Part 3: Channel geometry inside the chip

Describe channel geometry inside your microfluidic chip:



Rectangular channel*

Width w (μm)
200

Height h (μm)
1200

Length L (mm)
58

Part 4: Calculations

Select one information and fill your data to start calculations. Press enter to start and refresh calculations:

Flow rate fixed ($\mu\text{L/min}$) 0.29

Pressure fixed (mBar) 0.00e+0

Shear stress at wall τ fixed (dyn/cm^2) Shear stress (dyn/cm^2)
0.001

Fig. 2.8 Experimental parameters for microfluidic flow rate calculation (“Microfluidic Calculator,” Elveflow).

4. The microchips remained connected to the pump for a period of 1 day.
4. After microfluidic experiment, the microchips were disconnected from the pump and monitored again using „NIS-elements“ software following previous steps (2.6.1 – 2.6.4).

2.8 Statistical analysis

Following the data collection process, statistical analyses and calculations were conducted. Analyses were executed using the „SigmaPlot 14.5“ software program, facilitating statistical assessments of the collected data.

Data differences in cell density between three trials and different adhesion modifications (gelatin 38, gelatin 175, gelatin 300, collagen, gelatin 175/collagen mixtures) before and after microfluidic experiment were analyzed using one-way ANOVA and subsequent Student-Newman-Keuls (SNK) post-hoc test for comprehensive statistical evaluation.

3. RESULTS

3.1 Microchip production methodology improvements

After initial attempts using the old microchip production methodology yielded suboptimal results, areas for improvement were identified. Multiple microchips were fabricated, however, they exhibited side leakage, rendering them unsuitable for experimental use. Through iterative refinement, the production process was enhanced to address key challenges (Table 1).

Table 1. A comparison between the old and new methodology, highlighting the outcomes of these improvements.

Initial methodology	Updated methodology	Outcome
Old UV light source	New powerful UV light source with light path separator	Both UV light sources were custom-designed and fabricated in-house. The upgraded UV light source features a high-powered LED module with an optical power output of 1 W per single LED, significantly enhancing the efficiency of the curing process and reducing it 5 times. Additionally, the new UV light source incorporates a timer-based controller mechanism, enabling precise regulation of on/off cycles for optimal control over the curing process.
SLA mold heat curing	Extensive clean up after 3-D printing, SLA mold vacuum heat curing	SLA molds, particularly those designed for vertical surfaces, have demonstrated the capability to expedite mold curing processes and facilitate the removal of volatile organic compounds (VOCs), which subsequently promote higher PDMS curing rates around the outer perimeters of the mold.
PDMS mold usage 10 times	PDMS mold usage 5 times	Extended usage of OSTE in PDMS molds can lead to the accumulation of OSTE micro particles. Over time, this accumulation can result in the formation of larger clumps, hindering the successful removal of the OSTE from the mold.
Old mold design	New slim mold design with rounded edges and relief angles	A wider OSTE surface often cures with uneven high and low spots, while a slimmer design reduces such inconsistencies. Incorporating relief angles facilitates easier removal of PDMS from the printed master mold and OSTE from PDMS, ensuring the success rate of

		this step. Additionally, rounded edges facilitate effective air bubble escape during the pouring of OSTE polymer through the mold assembly.
Screw-based PDMS clamping system	Spring-based clamping system with a thickness stopper	This design allowed for more uniform clamping of PDMS against the glass surface during OSTE pouring, thereby maintaining a consistent thickness of OSTE across the substrate.
Plastic OSTE curing clamp system	Metal OSTE curing clamp system	The semi-cured or UV-cured OSTE possesses a sticky surface but a semi-hard internal structure, necessitating a high-pressure-withstanding clamping system. The metal system ensured a consistent clamping force at 60 °C, as the plastic one tended to deform after a few uses.
Manually glued luer ports onto COC substrates	Ordered COC substrates pre-fabricated with integrated ports	This change eliminated the need for manual port attachment, reducing assembly time and potential for adhesive-related issues, leading to more reliable and robust microchip performance
Clamping without spacer	Clamping with spacer (cardboard)	Using a spacer (cardboard) between COC slides ensured even distribution of clamping force around the microchannel and parallelism between COC slides. This resulted in uniform channel dimensions along the entire length of the microchip, preventing channel clogs due to OSTE displacement. Additionally, it prevented polycarbonate membranes from wrinkling and tearing, thus enhancing control over layer heights and promoting consistency in production.
Fabrication time 7-9 hours	Fabrication time 2-3 hours	Reduced fabrication time by 4-6 hours

These improvements have led to more efficient production processes, enhanced material performance, and greater consistency in the final microchip products (see suppl. 2). The optimization of this multi-step microchip fabrication process and creation of new fixtures resulted in a significant reduction in production time and enabled the simultaneous production of multiple chips, rather than one at a time, thus allowing for scaled-up microchip production. The iterative refinement of methodologies emphasizes the importance of continuous innovation and optimization in the field of microfluidic technology.

3.2 Microfluidic pump impact on glioma cell adhesion between trials

After fabricating the microfluidic chip, various solutions, including gelatin and collagen, were applied to modify its surface. To ensure an equal number of cells in each channel, one million cells were seeded onto the modified chip surface. Following cell seeding, a culture period of 6-7 days ensued within the microfluidic environment. The cellular adhesion and growth patterns were monitored using microscopy techniques before and after exposure to microfluidic pump-induced shear stress (at 0.001 dyn/cm²), allowing for comprehensive analysis of cell behavior under dynamic conditions. Cell density analysis was conducted on microscopy images, each representing a square area of 0.28 mm², captured using a 20x lens. From these standardized images, the density of both adherent and non-adherent cells was quantified.

Control group: Investigating glioma cell adhesion, significant differences were observed in cell counts per mm² of all trials between the control group adherent vs. non-adherent cells before microfluidic pump. In all trials, non-adherent cell counts were higher compared to adherent cells. The analysis revealed a statistically significant difference in cell counts of all trials among the treatment groups ($F(1.4) = 49.974$, $p = 0.002$). Post-hoc pairwise comparisons using the Student-Newman-Keuls method further confirmed significant differences between the cell counts of the control group adherent vs. non-adherent cells before microfluidic pump ($p < 0.05$). Specifically, the cell counts in 3 trial non-adherent cells was significantly higher than that in 3 trial adherent cells (Mean difference = 170.267, $p = 0.002$) (Fig. 3.1).

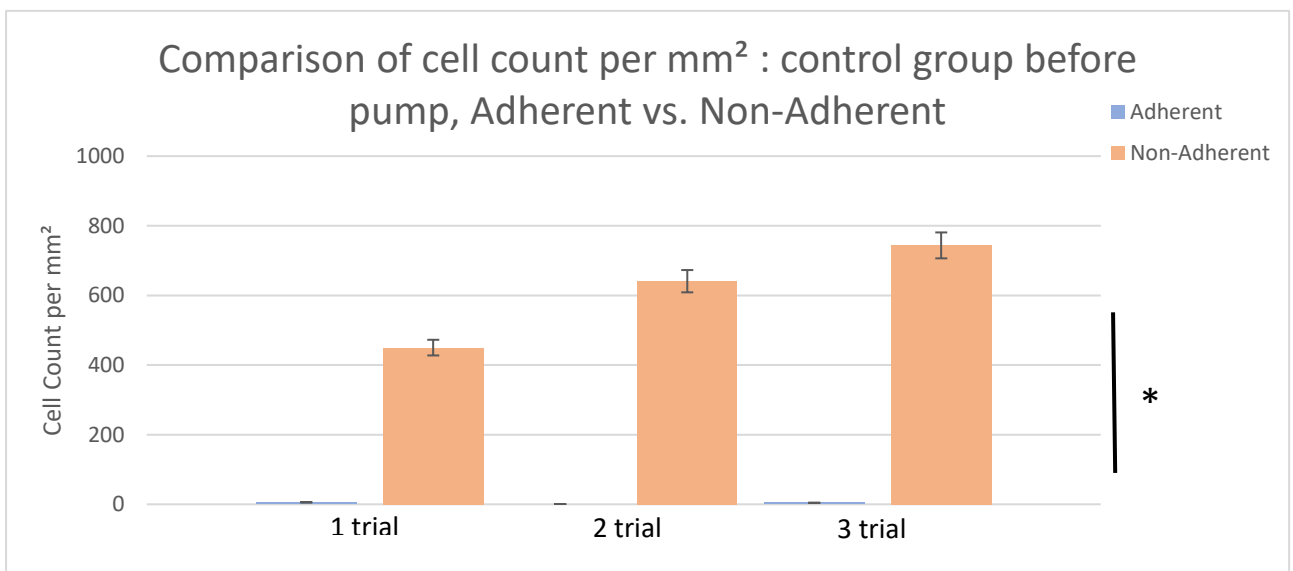


Fig. 3.1 Comparison of cell counts per mm² before microfluidic pump in the control group between 3 trials. The data are presented as means \pm S.E.M. „*“ indicating significant differences from the control group, $p < 0.05$.

These findings suggest that there are significant differences in cell adhesion of all trials between the control group before pump, with cell counts in 3 trial non-adherent cells exhibiting a significantly higher cell counts per mm² compared to 3 trial adherent cells.

Investigating the impact of a microfluidic pump on glioma cell adhesion, differences were observed in the cell counts per mm² of all trials between the control group adherent vs. non-adherent cells after microfluidic pump showing higher non-adherent cell counts compared to adherent cells. However, the differences in the cell counts among groups were not significant ($p = 0.100$), indicating that the observed variations could potentially be attributed to random sampling variability (Fig. 3.2).

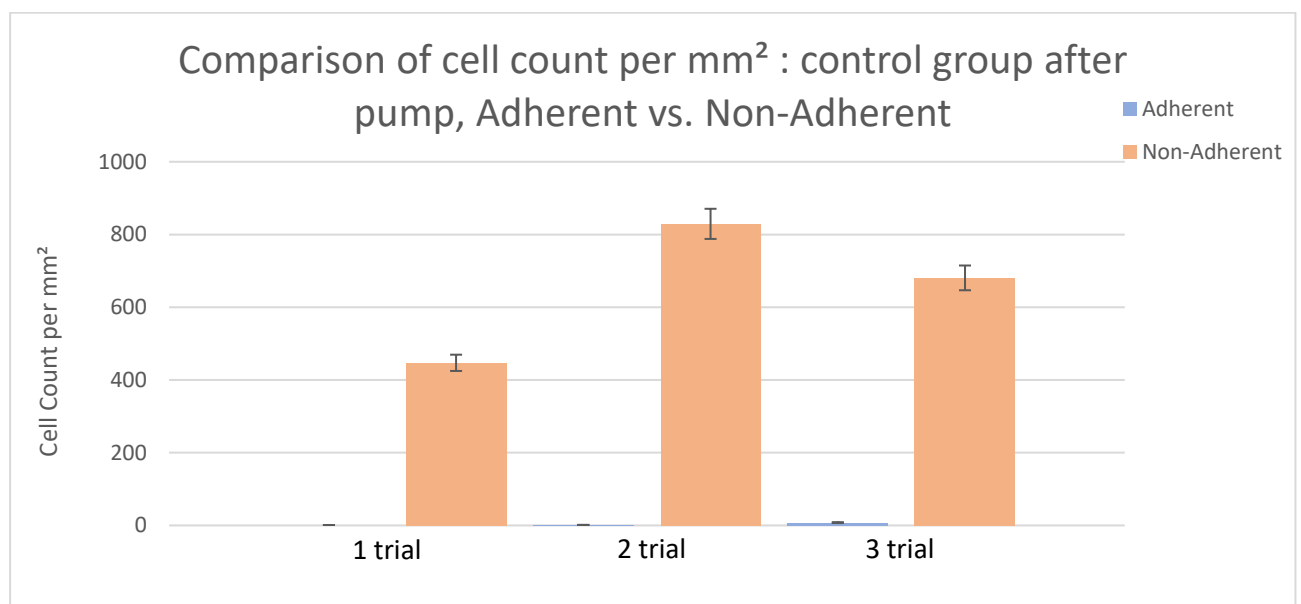


Fig. 3.2 Comparison of cell count per mm² before microfluidic pump in the control group between 3 trials. The data are presented as means \pm S.E.M.

These findings suggest that although there aren't significant differences in cell adhesion of all trials between the control group after pump, there is a pattern through all trials where non-adherent cell counts per mm² were higher.

Collagen group: Investigating glioma cell adhesion, significant differences were observed in the cell counts per mm² of all trials between the collagen group adherent vs. non-adherent cells before microfluidic pump. In all trials, non-adherent cell counts were higher compared to adherent cells. The analysis revealed a statistically significant difference in the cell counts of all trials among the treatment groups ($F(1, 4) = 9.971$, $p = 0.034$). Further pairwise comparisons using the Student-Newman-Keuls method indicated a significant difference in cell counts between non-adherent cells and adherent cells ($p = 0.034$) (Fig. 3.3).

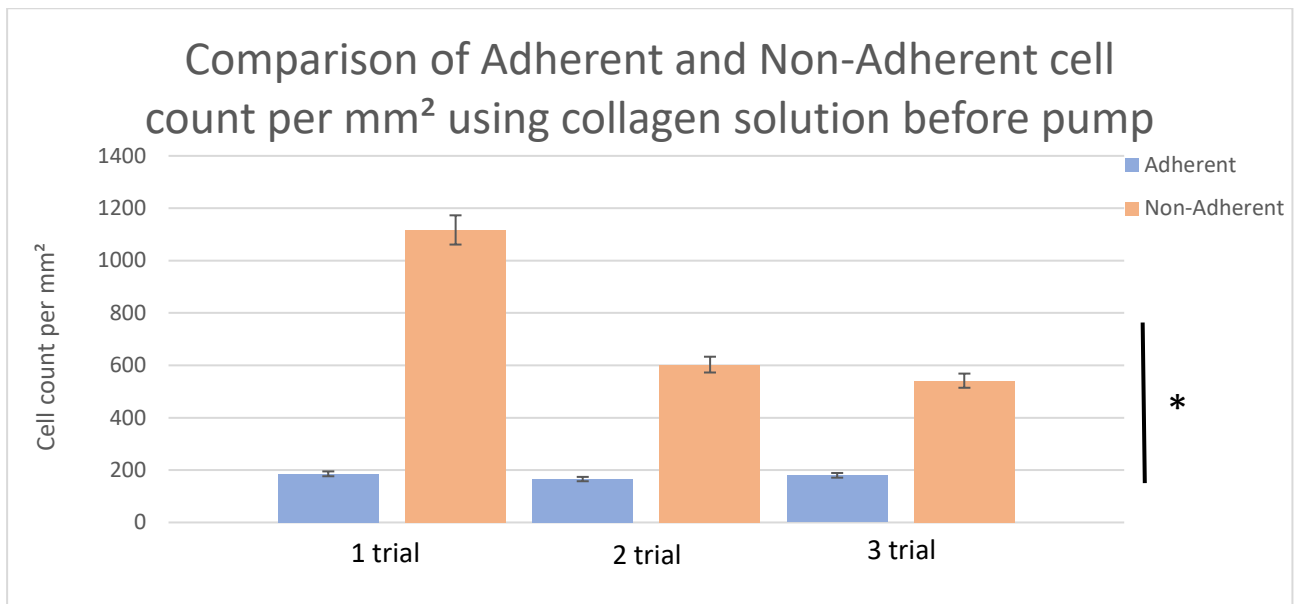


Fig. 3.3 Comparison of cell count per mm² before microfluidic pump in the collagen group between 3 trials. The data are presented as means \pm S.E.M. „*“ indicating significant differences from the control group, $p < 0.05$.

These findings suggest that there is a significant difference in the cell counts per mm² of adherent and non-adherent cells between the collagen groups before the pump. This could imply that the collagen treatment may have influenced the adhesion properties of the glioma cells, leading to a higher proportion of cells remaining non-adherent under the experimental conditions.

The data from the collagen group after the pump was subjected showed significant differences in the cell counts per mm² of all trials between the adherent vs. non-adherent cells. In all trials, non-adherent cell counts were higher compared to adherent cells. The analysis revealed a statistically significant difference in cell counts of all trials among the treatment groups ($F(1.4) = 37.304$, $p = 0.004$). Further pairwise comparisons using the Student-Newman-Keuls method indicated a significant difference in cell counts between non-adherent cells and adherent cells ($p = 0.004$) (Fig. 3.4).

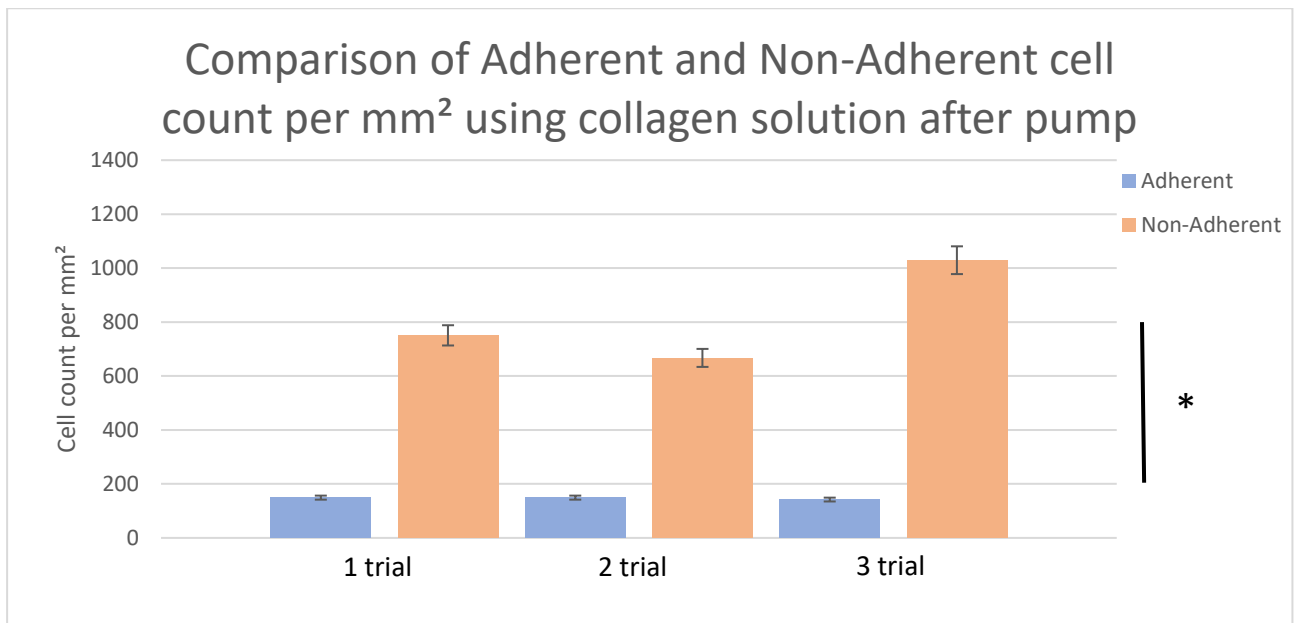


Fig. 3.4 Comparison of cell counts per mm² after microfluidic pump in the collagen group between 3 trials. The data are presented as means \pm S.E.M. „*“ indicating significant differences from the control group, $p < 0.05$.

These results indicate that there is a statistically significant difference in the collagen-treated group cell counts per mm² between non-adherent and adherent cells after the pump. Specifically, non-adherent cell counts in the collagen-treated group is significantly higher compared to the adherent cell counts in the collagen-treated group. This suggests that the collagen treatment may have influenced the adhesion properties of glioma cells, leading to a higher number of non-adherent cells after exposure to the microfluidic pump.

Gelatin 38: Investigating glioma cell adhesion, differences were observed in the cell counts per mm² of all trials between the gelatin 38 group adherent vs. non-adherent cell counts before microfluidic pump showing higher non-adherent cell counts compared to adherent cells in 2 and 3 trial. However, these results suggest that there is not a statistically significant difference in the cell counts of adherent vs. non-adherent cells between the gelatin 38 treated group ($p = 0.246$) (Fig. 3.5).

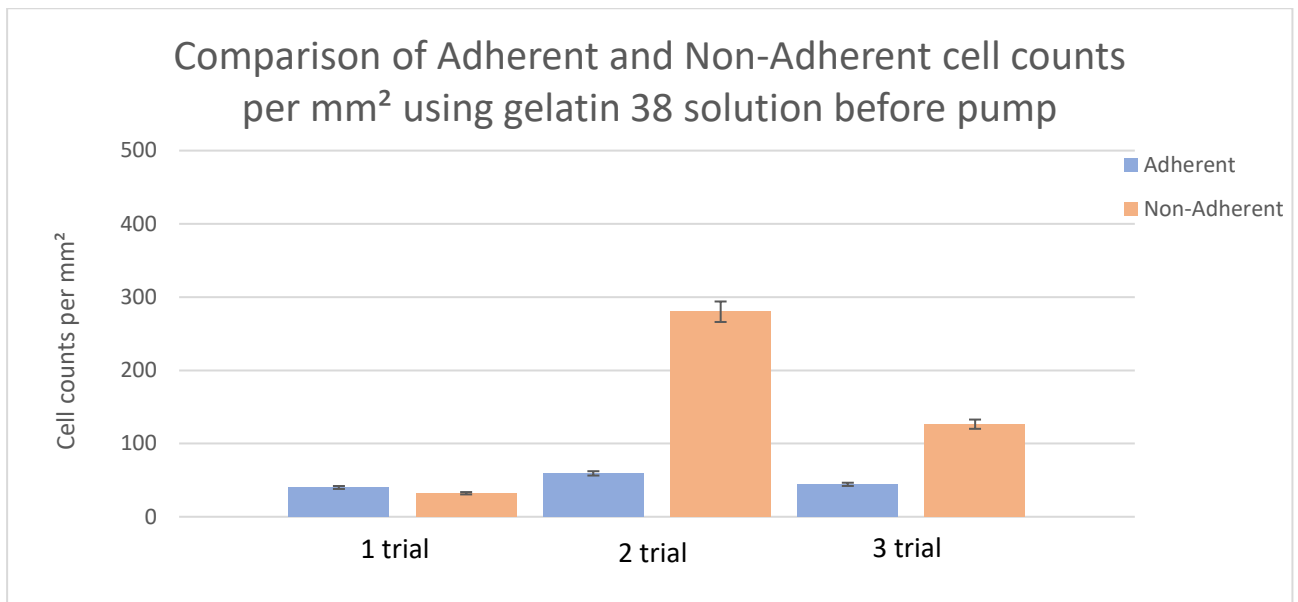


Fig. 3.5 Comparison of cell counts per mm² before microfluidic pump in the gelatin 38 treatment group between 3 trials. The data are presented as means \pm S.E.M.

After microfluidic pump was introduced differences were observed in the cell counts per mm² of all trials between the gelatin 38 group adherent vs. non-adherent cells showing higher non-adherent cell counts compared to adherent cells in all trials. However, these results suggest that there is not a statistically significant difference in the cell counts of adherent vs. non-adherent cells between the gelatin 38 treated group ($p = 0.100$) (Fig. 3.6).

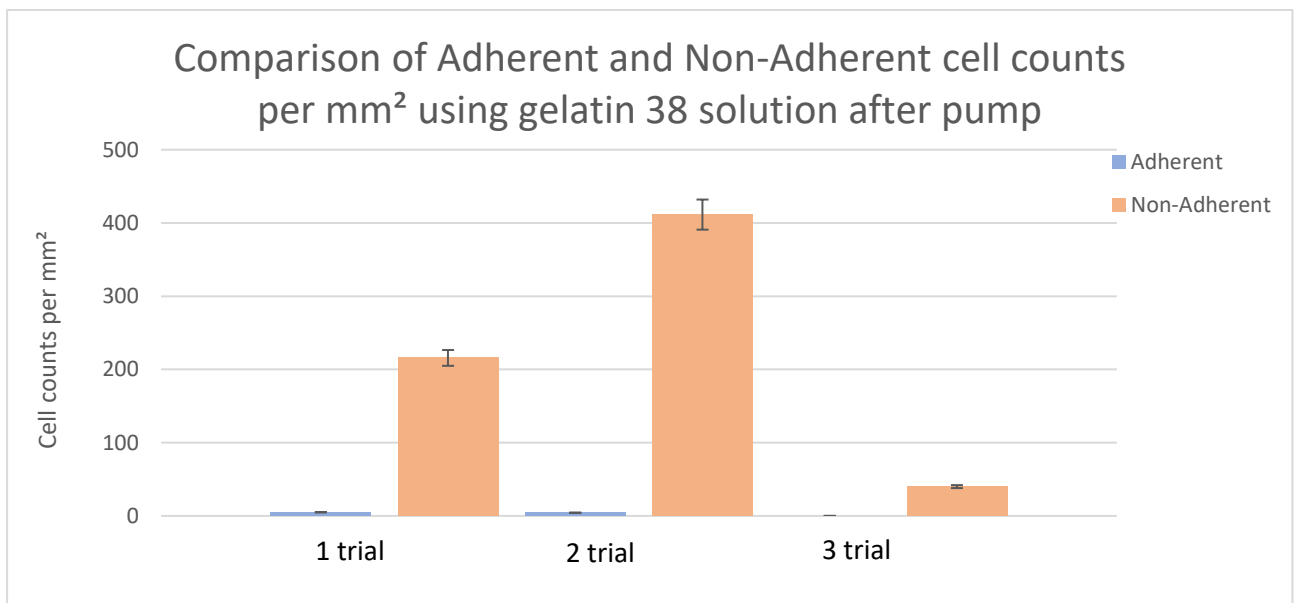


Fig. 3.6 Comparison of cell counts per mm² after microfluidic pump in the gelatin 38 treatment group between 3 trials. The data are presented as means \pm S.E.M.

Although there were not a statistically significant difference in the cell counts per mm² of adherent vs. non-adherent cells between the gelatin 38 treated group, a pattern of higher non-adherent cell

counts between all trials could be seen. These findings would indicate, that gelatin 38 treatment may have influenced the adhesion properties of glioma cells, leading to a higher number of non-adherent cells after exposure to the microfluidic pump.

Gelatin 175: Investigating glioma cell adhesion, differences were observed in the cell counts per mm² of all trials between the gelatin 175 group adherent vs. non-adherent cells before microfluidic pump showing higher non-adherent cell counts. However, these results suggest that there is not a statistically significant difference in the cell counts of adherent vs. non-adherent cells between the gelatin 175 treated group ($p = 0.100$) (Fig. 3.7).

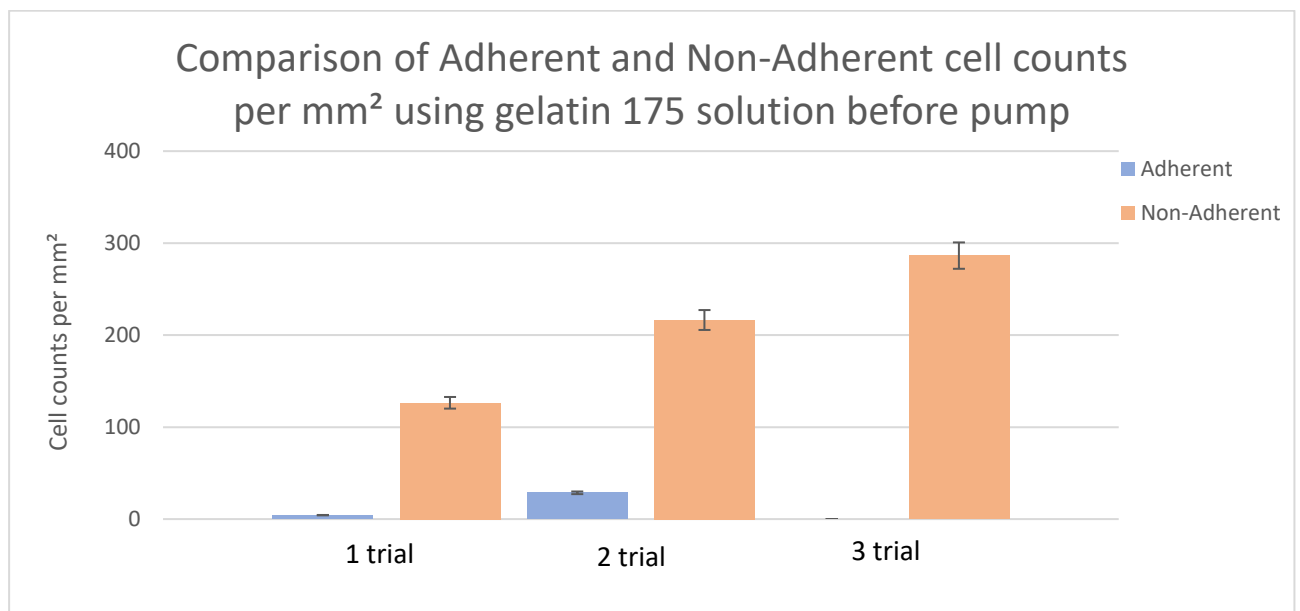


Fig. 3.7 Comparison of cell counts per mm² before microfluidic pump in the gelatin 175 treatment group between 3 trials. The data are presented as means \pm S.E.M.

Although there were not a statistically significant difference in the cell counts per mm² of adherent vs. non-adherent cells between the gelatin 175 treated group, a pattern of higher non-adherent cells between all trials could be seen. These findings would indicate, that gelatin 175 treatment may have influenced the adhesion properties of glioma cells, leading to a higher number of non-adherent cells.

The data from the gelatin 175 group after the pump was subjected showed significant differences in the cell counts per mm² of all trials between the adherent vs. non-adherent cell counts. In all trials, non-adherent cell counts were higher compared to adherent cells. The analysis revealed a statistically significant difference in cell counts of all trials among the treatment groups ($F(1, 4) = 121.223, p < 0.001$). Further pairwise comparisons using the Student-Newman-Keuls method indicated a significant difference in cell counts between non-adherent cells and adherent cells ($p < 0.001$) (Fig. 3.8).

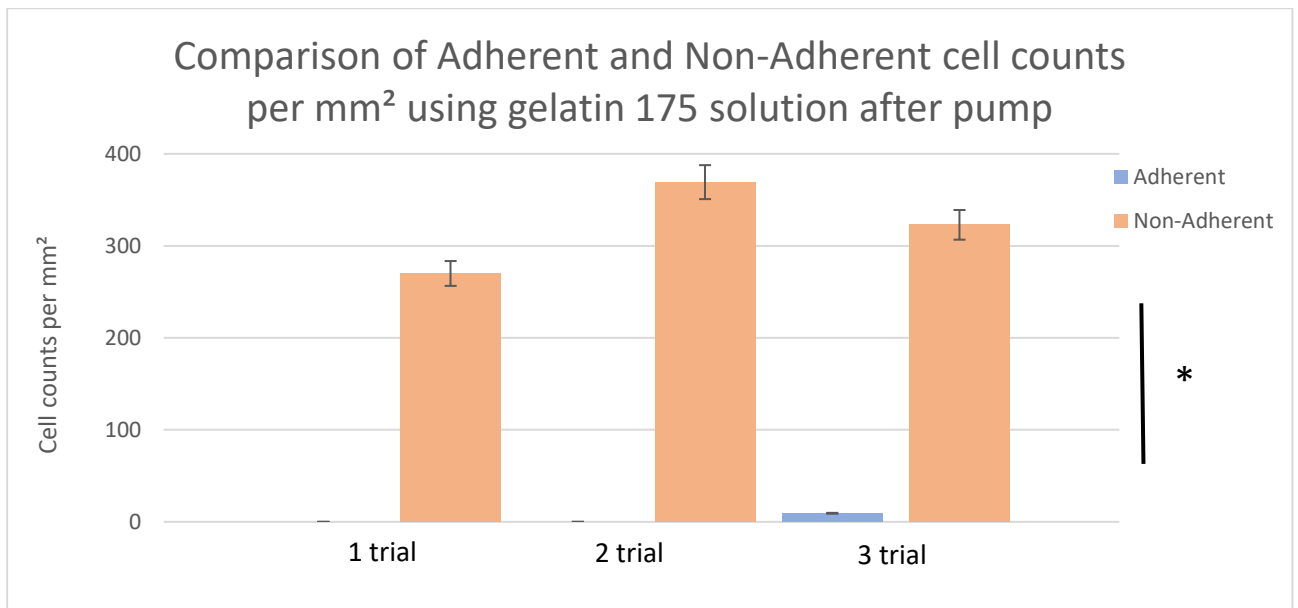


Fig. 3.8 Comparison of cell counts per mm² after microfluidic pump in the gelatin 175 group between 3 trials. The data are presented as means \pm S.E.M. „*“ indicating significant differences from the control group, $p < 0.001$.

These results indicate that there is a statistically significant difference in the gelatin 175 treated group cell counts per mm² between non-adherent and adherent cells after the pump. Specifically, cell counts per of non-adherent cells in the gelatin 175 treated group is significantly higher compared to the adherent cells. This suggests that the gelatin 175 treatment may have influenced the adhesion properties of glioma cells, leading to a higher number of non-adherent cells after exposure to the microfluidic pump.

Gelatin 300: Investigating glioma cell adhesion, significant differences were observed in the cell counts per mm² of all trials between the gelatin 300 group adherent vs. non-adherent cells before microfluidic pump. In all trials, non-adherent cell counts were higher compared to adherent cells. The analysis revealed a statistically significant difference in cell counts of all trials among the treatment groups ($F(1, 4) = 13.624$, $p = 0.021$). Further pairwise comparisons using the Student-Newman-Keuls method indicated a significant difference in cell counts per between non-adherent cells and adherent cells ($p = 0.021$) (Fig. 3.9).

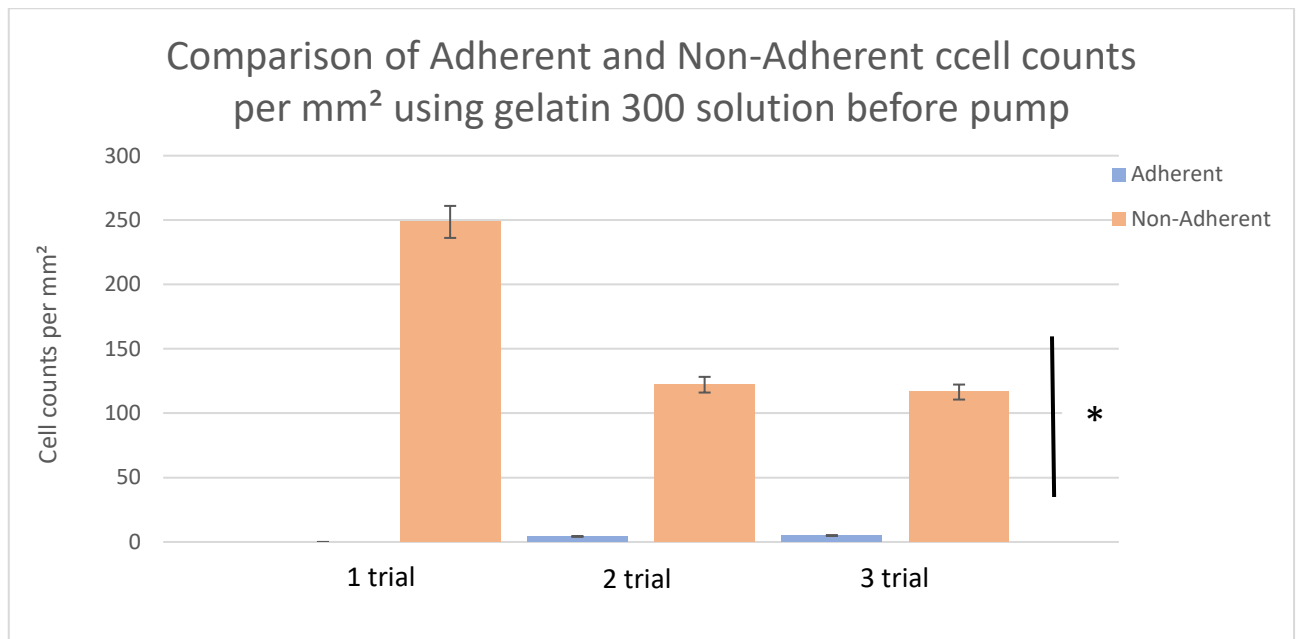


Fig. 3.9 Comparison of cell counts per mm² before microfluidic pump in the gelatin 300 group between 3 trials. The data are presented as means \pm S.E.M. „*“ indicating significant differences from the control group, $p < 0.05$.

These findings suggest that there is a significant difference in the cell counts per mm² of adherent and non-adherent cells between the gelatin 300 groups before the pump. This could imply that the gelatin 300 treatment may have influenced the adhesion properties of the glioma cells, leading to a higher proportion of cells remaining non-adherent under the experimental conditions.

The data from the gelatin 300 group after the pump was subjected showed significant differences in the cell counts per mm² of all trials between the adherent vs. non-adherent cells. In all trials, non-adherent cell counts were higher compared to adherent cells. The analysis revealed a statistically significant difference in cell counts of all trials among the treatment groups ($F(1.4) = 11.664$, $p = 0.027$). Further pairwise comparisons using the Student-Newman-Keuls method indicated a significant difference in cell counts between non-adherent cells and adherent cells ($p = 0.027$) (Fig. 3.10).

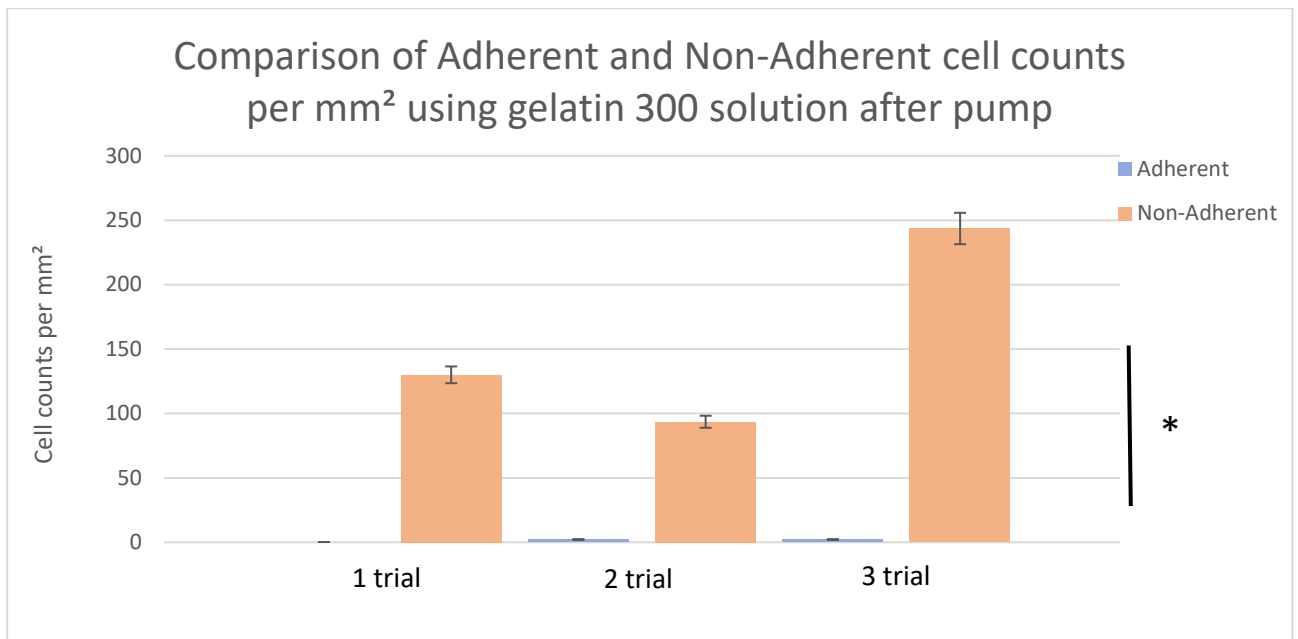


Fig. 3.10 Comparison of cell counts per mm² after microfluidic pump in the gelatin 300 group between 3 trials. The data are presented as means \pm S.E.M. „*“ indicating significant differences from the control group, $p < 0.05$.

These results indicate that there is a statistically significant difference in the gelatin 300 treated group cell counts per mm² between non-adherent and adherent cells after the pump. Specifically, the non-adherent cell counts in the gelatin 300 treated group is significantly higher compared to the adherent cells. This suggests that the gelatin 300 treatment may have influenced the adhesion properties of glioma cells, leading to a higher number of non-adherent cells after exposure to the microfluidic pump.

Mix: Investigating glioma cell adhesion, significant differences were observed in the cell counts per mm² of all trials between the mix (collagen/gelatin 175) group adherent vs. non-adherent cells before microfluidic pump. In all trials, non-adherent cell counts were higher compared to adherent cells. The analysis revealed a statistically significant difference in cell counts of all trials among the treatment groups ($F(1.4) = 38.604$, $p = 0.003$). Further pairwise comparisons using the Student-Newman-Keuls method indicated a significant difference in cell counts between non-adherent cells and adherent cells ($p = 0.003$) (Fig. 3.11).

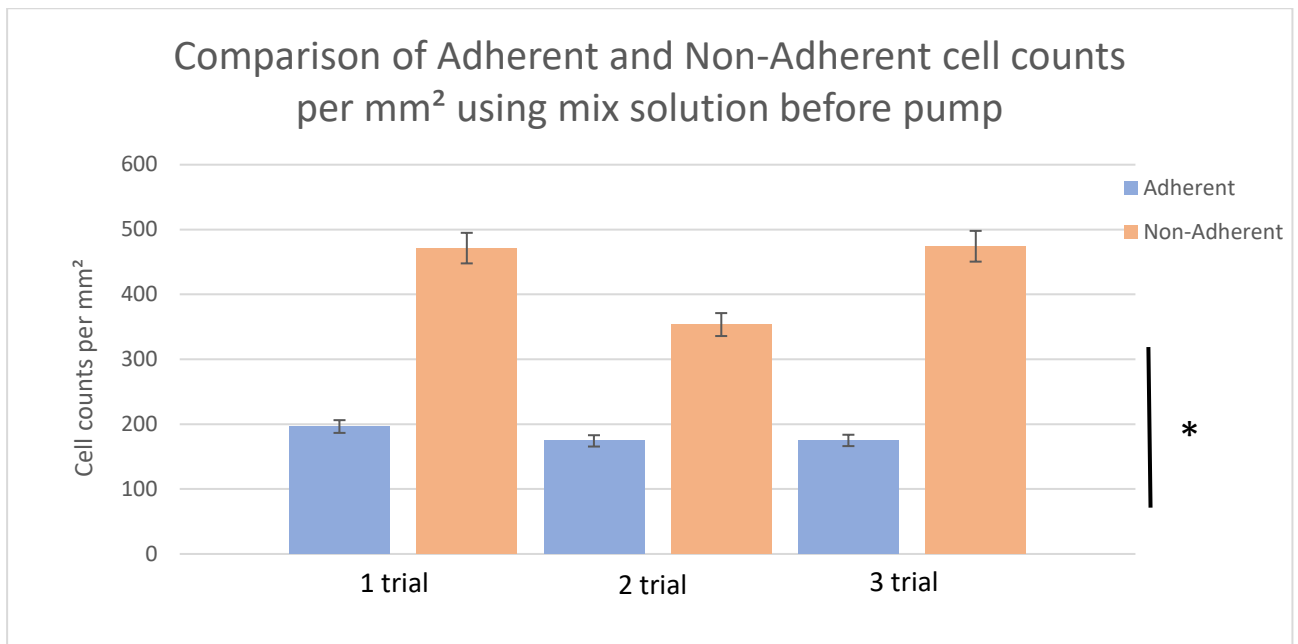


Fig. 3.11 Comparison of cell counts per mm² before microfluidic pump in the mix group between 3 trials. The data are presented as means \pm S.E.M. „*“ indicating significant differences from the control group, $p < 0.05$.

These findings suggest that there is a significant difference in the cell counts per mm² of adherent and non-adherent cells between the mix groups before the pump. This could imply that the mix treatment may have influenced the adhesion properties of the glioma cells, leading to a higher proportion of cells remaining non-adherent under the experimental conditions.

The data from the mix group after the pump was subjected showed significant differences in the cell counts per mm² of all trials between the adherent vs. non-adherent cells. In all trials, non-adherent cell counts were higher compared to adherent cells. The analysis revealed a statistically significant difference in cell counts of all trials among the treatment groups ($F(1.4) = 89.907, p < 0.001$). Further pairwise comparisons using the Student-Newman-Keuls method indicated a significant difference in cell counts between non-adherent cells and adherent cells ($p < 0.001$) (Fig. 3.12).

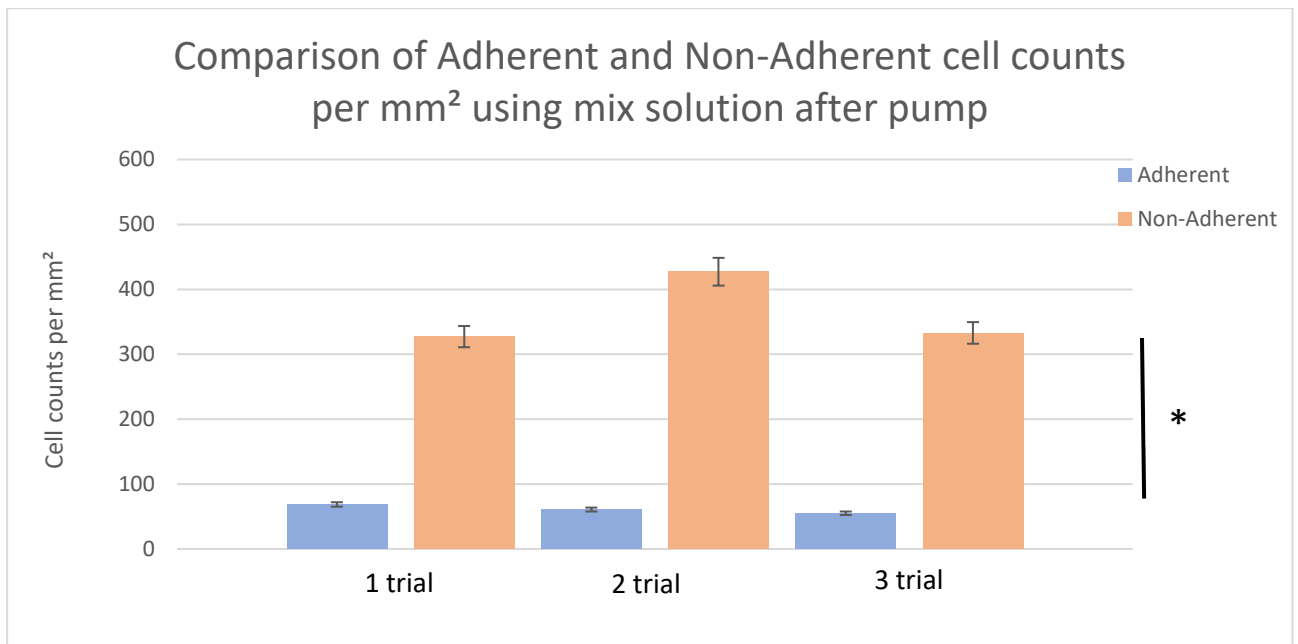


Fig. 3.12 Comparison of cell counts per mm² after microfluidic pump in the mix group between 3 trials. The data are presented as means \pm S.E.M. „*“ indicating significant differences from the control group, $p < 0.001$.

These results indicate that there is a statistically significant difference in the mix treated group cell counts per mm² between non-adherent and adherent cells after the pump. Specifically, the cell counts of non-adherent cells in the mix treated group is significantly higher compared to the adherent cells. This suggests that the mix treatment may have influenced the adhesion properties of glioma cells, leading to a higher number of non-adherent cells after exposure to the microfluidic pump.

In conclusion, the results revealed that collagen and mixed (collagen/gelatin 175) substrates showed higher cell adhesion compared to gelatin 38, gelatin 175, gelatin 300, and control solutions in the microfluidic chip model. However, introduction of the microfluidic pump consistently resulted in the detachment of adherent cells.

3.3 Microfluidic pump impact on glioma cell adhesion between different adhesion modification methods

Cell density analysis was conducted on microscopy images, each representing a square area of 0.28 mm², captured using a 20x lens. From these standardized images, the density of adherent cells of different adhesion modification methods was quantified.

Adherent cell counts between different adhesion modification methods: Data from previous trials was consolidated to compare the efficacy of different adhesion modification methods. Investigating the impact of a microfluidic pump on glioma cell adhesion, differences were observed in the cell counts per mm² of various adhesion modification methods. However, these results suggest

that there is not a statistically significant difference in the cell counts of adherent cell counts ($p = 0.960$) (Fig. 3.13).

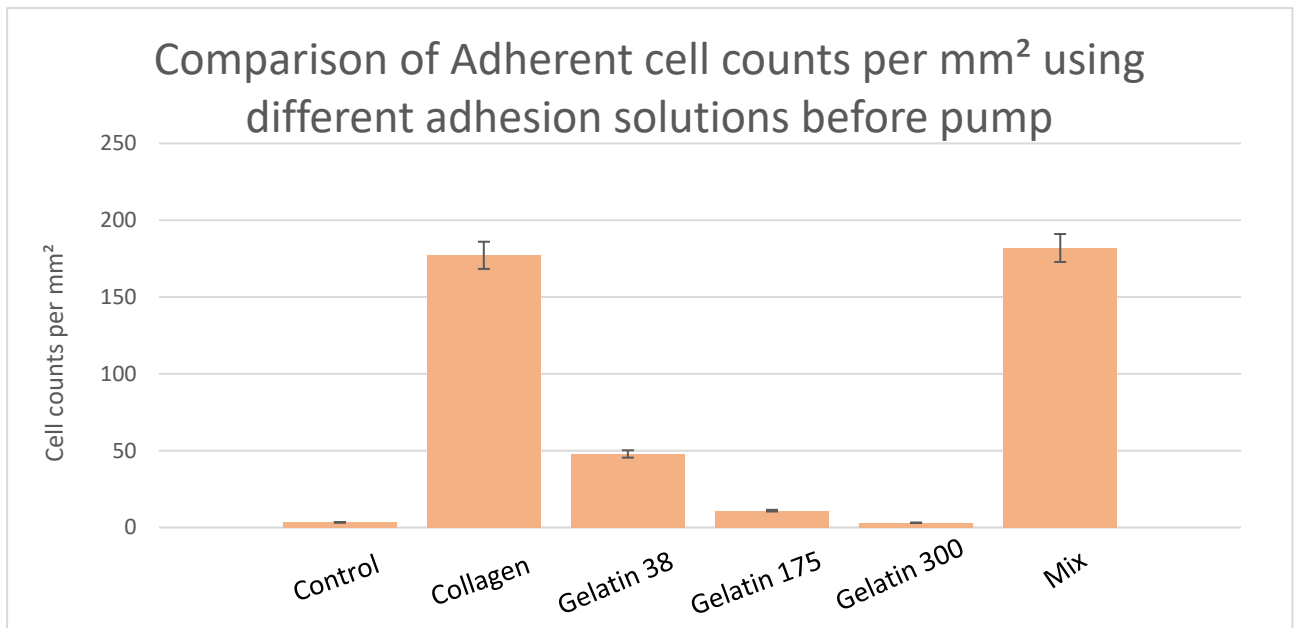


Fig. 3.13 Comparison of adherent cell counts per mm² using different adhesion solutions before pump. The data are presented as means \pm S.E.M.

Nevertheless, higher adherent cell counts could be seen in collagen and mix modification methods. This could suggest that collagen and mix modification methods can increase cell adhesion in further experiments with developed microchip.

Investigating the impact of a microfluidic pump on glioma cell adhesion, differences were observed in the cell counts per mm² of various adhesion modification methods. However, these results suggest that there is not a statistically significant difference in the cell counts of adherent cells ($p = 0.834$) (Fig. 3.14).

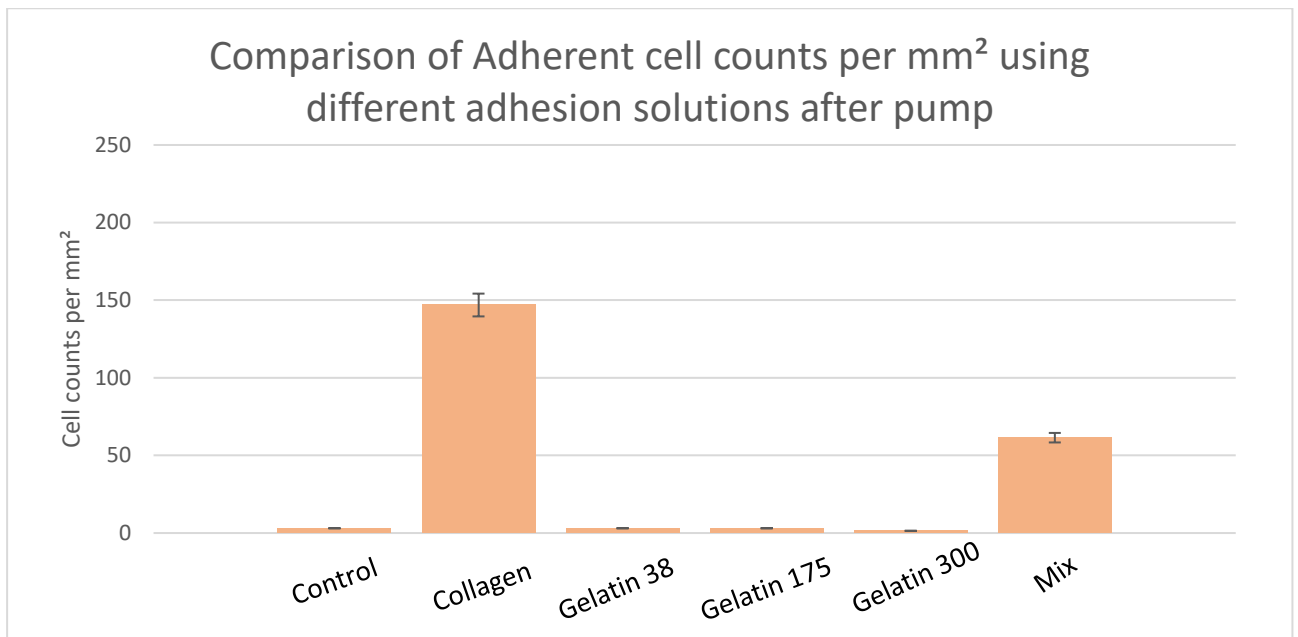


Fig. 3.14 Comparison of adherent cell counts per mm² using different adhesion solutions after pump. The data are presented as means ± S.E.M.

Nevertheless, higher adherent cell counts could be seen in collagen and mix modification methods, especially in collagen modification method. This could suggest that collagen can increase cell adhesion.

The percentage of adherent cells after the introduction of the microfluidic pump was analyzed to assess the impact of different adhesion modification methods. The data revealed distinct variations in the retention of adherent cells across various modification techniques (Fig. 3.15).

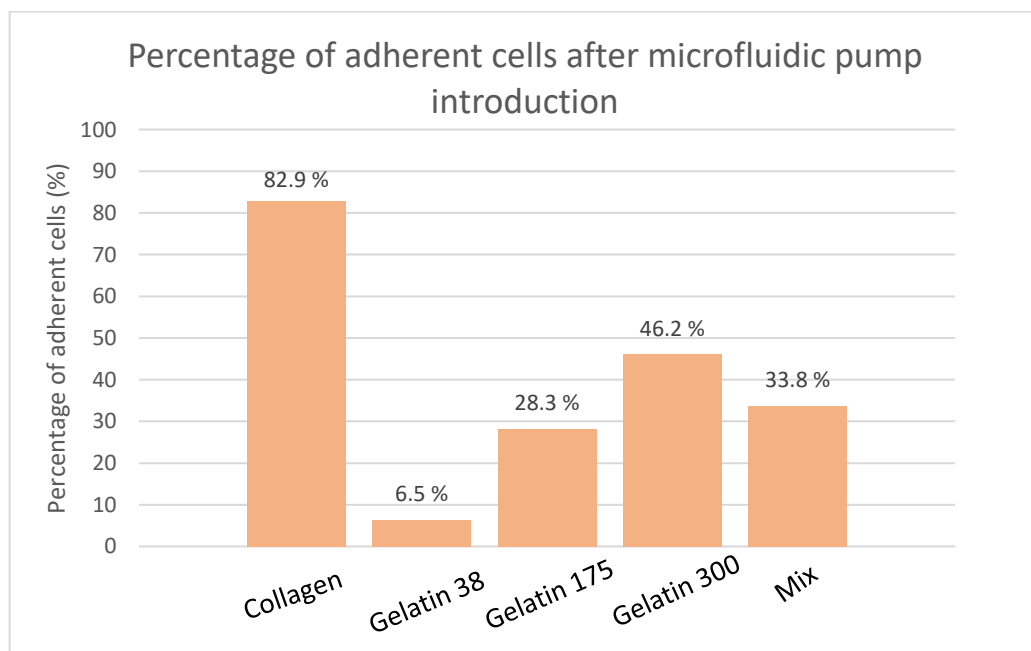


Fig. 3.15 Percentage of adherent cells after microfluidic pump introduction of different adhesion solutions.

Collagen demonstrated the highest percentage (82.9 %) of adherent cells after the introduction of the microfluidic pump, consistent with previous findings, however, the relatively high percentage of adherent cells for gelatin 300 (46.2 %) after the introduction of the microfluidic pump may be attributed to the lower overall number of cells adhering to gelatin compared to collagen before the pump was introduced. While gelatin 300 showed lower absolute counts of adherent cells, the percentage decrease after pump exposure appears higher due to the smaller initial cell proliferation, resulting in a comparatively higher percentage. Mix (33.8%) method, similar to collagen, had relatively high percentage, which was consistent with its initial higher cell counts. Gelatin 38 (6.5 %) and gelatin 175 (28.3 %), having the smallest initial cell counts, consequently exhibited the smallest percentages post-pump exposure.

4. DISCUSSION

Malignant gliomas represent the predominant form of primary brain tumors, with glioblastoma multiforme (GBM) ranking as the most aggressive subtype classified as grade IV glioma by the World Health Organization (WHO) (Diao et al., 2019). Despite comprehensive treatment involving surgical resection, radiation therapy, and chemotherapy, GBM patients typically face a median life expectancy of merely 12–15 months. Notably, GBMs exhibit a propensity for recurrence within close proximity to the original tumor site, a phenomenon largely attributed to the diffuse invasion of GBM cells into adjacent brain tissue. Understanding the mechanisms underlying this invasive behavior is paramount for the development of effective therapeutic interventions (Furnari et al., 2007). Given that *in vivo* animal models are complex, expensive, time consuming, various *in vitro* models have been constructed to further study the complex interactions between GBM cells and ECM. Cells grown in traditional two-dimensional (2-D) setups react quickly to changes in their surroundings, but these settings don't accurately mimic the *in vivo* microenvironment. Three-dimensional (3-D) models are better suited for studying conditions like GBMs (Cha and Kim, 2017). For instance, neurosphere cultures created from freshly isolated GBM cells maintain stemness and form semi-3-D models, though they require longer preparation. To mimic the *in vivo* environment more effectively, researchers use natural hydrogels like collagen as substitutes for native ECM *in vitro* models. These 3-D models allow for the study of cell invasion through native ECM by replicating nutrient and oxygen diffusion through tissue (Kaufman et al., 2005). In a study by Diao et al. the interaction between GBMs and ECM using four types of GBM cells lines (LN229, SNB19, U251, U87) with origin from neuroepithelial cells were cultured in a micro-fabricated 3-D *in vitro* model. The micro-structured chips in the model were constructed to possess an array of 3-D hollow micro-chambers embedded in collagen I gel so as to enable simultaneous investigation of GBM cells proliferation, migration, and invasion in a suitable microenvironment. Results showed variations in morphology and behavior among different cell lines, with U87 cells forming clusters, LN229 cells displaying triangular or diamond shapes, and varying proliferation rates among cell lines. Additionally, U87 cells demonstrated the highest migration speed and invasion ability, characterized by long protrusions into surrounding collagen, while SNB19 cells exhibited single-cell invasion, and LN229 and U251 cells showed less invasion. Findings of this study would suggest that different GBM cell lines exhibit distinct morphological characteristics, proliferation rates, migration speeds, and invasion abilities and collagen served as a crucial component in this study by providing a substrate for the GBM cells to grow and interact with. The use of collagen allowed for the creation of an *in vitro* model that mimicked aspects of the extracellular matrix found *in vivo*, providing a more physiologically relevant microenvironment for studying cell behavior, including migration and invasion (Diao et al., 2019).

The aim of the experiment was to fabricate a microfluidic chip for the investigation of the adhesion behavior of C6 rat glioma cells under different extracellular matrix conditions, including various gelatin concentrations, collagen, and control substrates. Through iterative refinement, the fabrication process evolved, integrating an array of methodologies and materials aimed at optimizing chip production. This comprehensive approach encompassed meticulous adjustments and explorations, such as UV light source, SLA mold heat curing, PDMS mold, PDMS clamping system, OSTE curing clamp system, and COC substrates, each contributing to the enhancement of the fabrication process. Ultimately, this led to the production of an optimized microfluidic chip. The multi-step fabrication process involved 3-D printing of master molds, casting of PDMS molds, preparation of COC substrates, and injection casting of a photo-curable resin – OSTE. Polycarbonate membranes were prepared and placed onto the COC substrates following oxygen plasma treatment. Finally, the microfluidic chip was constructed by assembling COC substrates with patterned relief structures, ensuring precise alignment and integration of components essential for cell adhesion studies. The optimization of this multi-step microchip fabrication process resulted in a significant reduction in a production time, from 8 hours to 2 hours, thereby enhancing manufacturing efficiency. Additionally, through the creation of new fixtures and manufacturing systems, the improvements now enable the simultaneous production of multiple chips, rather than one at a time, thus allowing for scaled-up microchip production.

The development of the microfluidic chip was essential for advancing the understanding of C6 glioma cell adhesion under varying extracellular matrix conditions, providing a controlled environment to systematically study cell responses and demonstrating the potential of this research for simulating complex cellular interactions in microenvironments. Lu et al. developed microfluidic devices designed for studying fibroblast cell line WT NR6 cell adhesion and mechanics. In the experiment microfluidic channel was coated with different concentrations of fibronectin molecules from solutions and shear stress was increased from 0 to 1600 dyn/cm² through step increases in the buffer flow rate at discrete time intervals to sample increasing levels of force response. Results showed that the strongest cell adhesion was detected when channel was coated with highest concentration of fibronectin (10 µg/mL), with only ~10% of cells distracted at the maximal shear stress value of 1600 dyn/cm². However, to capture the dynamic cell detachment profile effectively, much higher shear stress was applied. By coating microfluidic channels with varying concentrations of fibronectin and applying stepwise increases in shear stress, the study systematically sampled force responses, enabling a comprehensive analysis of cell adhesion dynamics under different mechanical stimuli in the microfluidic chip (Lu et al., 2004). These findings confirm an innovative approach that allows integration of multiple experimental parameters, facilitating comprehensive analyses of cell

adhesion mechanisms and highlighting the significance of microfluidic platforms in advancing cell biology research.

The experiment commenced with the fabrication of microfluidic chips conducive to cell culture. Gelatin solutions of varying concentrations (gelatin 175, gelatin 80, gelatin 300), collagen solution, mix solution of gelatin 175/collagen (with ratio 1:1, respectively) and control substrates were prepared. Subsequently, these solutions were injected into the channels of the microfluidic chips. One million of C6 glioma cells were then seeded onto the surfaces of the microfluidic chips containing the different substrates, to ensure an equal number of cells in each channel. Over the course of approximately one week, the cells were cultured within the microfluidic environment. Imaging of the cells using microscope was performed both before and after exposure to fluid flow from the pump. Through meticulous analysis, the adhesion behavior of the C6 glioma cells was assessed, with a particular focus on quantifying adherent and non-adherent cells between trials and different adhesion modification methods. Finally, statistical analysis of the data was conducted to elucidate the effects of the various substrates on C6 glioma cell adhesion within the controlled microfluidic setting.

The investigation into the impact of a microfluidic pump on C6 glioma cell adhesion revealed compelling variations in mean cell counts between adherent and non-adherent cells within each treatment group both before and after exposure to the microfluidic environment. Notably, in the control group, significant disparities were evident, with consistently higher non-adherent cell counts observed across all trials. However, following exposure to the pump, while non-adherent cell counts remained consistently elevated, the differences failed to achieve statistical significance, suggesting potential fluctuations in adhesion dynamics (Fig. 3.1 – 3.2). Similarly, in the collagen, gelatin 38, gelatin 175, gelatin 300, and mix groups, significant differences in mean cell counts were discerned before and after the pump, with non-adherent cell counts prevailing (Fig. 3.3 – 3.12). These findings strongly suggest that the adhesion properties of C6 glioma cells may be modulated by the treatment administered, with certain substrates – gelatin 38, gelatin 175, gelatin 300 potentially fostering increased non-adherent cell populations subsequent to exposure to microfluidic conditions. Furthermore, the results from the investigation into the impact of a microfluidic pump on C6 glioma cell adhesion between different adhesion modification methods revealed interesting findings. Despite observing differences in the mean cell counts of various adhesion modification methods, statistical analysis indicated that there was not a significant difference in the mean values of adherent cell counts before the pump ($p = 0.960$) (Fig. 3.13). However, higher adherent cell counts were evident in collagen and mix modification methods, hinting at the potential of these methods to enhance cell adhesion. Following the introduction of the microfluidic pump, similar trends were observed in the mean cell counts of various adhesion modification methods, with no statistically significant

difference noted ($p = 0.834$) (Fig. 3.14). Notably, collagen and mix modification methods still exhibited higher adherent cell counts, particularly the collagen modification method resulting in 82.9% of cells remaining adherent to the surface after the introduction of the microfluidic pump (Fig. 3.15). This reaffirms the notion that collagen may play a crucial role in promoting cell adhesion, as evidenced by the consistently higher counts observed across both experimental phases. These findings underscore the importance of considering the choice of adhesion modification methods when designing microfluidic systems for studying cell adhesion. In contrast, Cai et al. presented gelatin usage for cell adhesion, where gelatin microspheres were shown to support the growth of highly viable HepG2 cells (Cai et al., 2020). Similar results were observed in the study performed by Song and Jang, where plates coated with gelatin showed increased embryonic stem cell adhesion on the surface (Song and Jang, 2023). The observed decrease in C6 glioma adherent cell counts with different types of gelatin may include variations in gelatin concentration, surface treatment methods, and experimental conditions such as flow rates or shear stresses. Additionally, there were observed gelatin bubbles from cell pictures taken by microscope (Fig. 4.1).

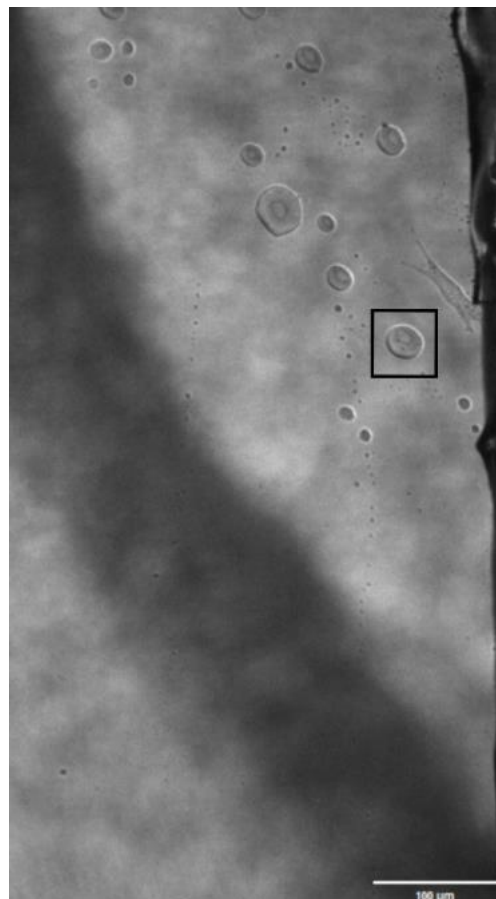


Fig. 4.1 Gelatin bubbles observed on the surface of the substrate. Scale bar: 100 μm . (Photo courtesy of the author).

These bubbles might have created irregularities or barriers, impeding the proper adhesion of cells. This observation underscores the importance of ensuring a smooth and uniform surface for cell attachment in microfluidic experiments. Further optimization of the gelatin coating process may be necessary to mitigate these effects and enhance cell adhesion within the microfluidic system. However, observed increase in C6 glioma adherent cell counts with collagen and mix of collagen and gelatin 175 was consistent with findings reported in various studies. Wu et al., presented a study investigating the influence of polyvinyl alcohol (PVA) substrates blended with different concentration of collagen or/and gelatin on the cell adhesion, proliferation, shape, spreading, and differentiation of stem cells. Results have showed, that collagen or/and gelatin blended PVA substrates showed enhanced NIH-3T3 fibroblast adhesion as comparing with the pure PVA (I.-C. Wu et al., 2023). In another study performed by Li et al., cell adhesion and proliferation of adipose-derived stromal cells (ADSCs) modified with collagen was evaluated and results have shown enhanced adhesion of cultured ADSCs on the scaffold (X. Li et al., 2008).

In conclusion, investigation into the impact of a microfluidic pump on C6 glioma cell adhesion revealed significant variations in cell counts across different adhesion modification methods. Collagen and mix of collagen/gelatin 175 modification methods emerged as a prominent adhesion promoter, exhibiting higher adherent cell counts, consistent with previous studies. However, gelatin solutions exhibited a reduction in C6 glioma adherent cell counts. The presence of gelatin bubbles observed on the substrate surface may have contributed to the observed decrease in cell adhesion, highlighting the need for further optimization of gelatin coating processes. Collagen's role as an adhesion promoter for these cells is highlighted, while gelatin, though ineffective alone, does not interfere when combined in the mix solution. This suggests the potential to develop adhesive systems where collagen serves as the adhesion promoter, with another material acting as a matrix or polymer coating compound. Nonetheless, these findings underscore the importance of carefully selecting adhesion modification methods in microfluidic systems to facilitate robust cell adhesion studies and advance understanding of cellular behavior in controlled microenvironments.

5. CONCLUSIONS

1. Optimization of the multi-step microchip fabrication process resulted in a significant reduction in production time, from 8 hours to 2 hours, thereby enhancing manufacturing efficiency.
2. Created manufacturing subsystems and fixtures allowed microchip production to be scaled up, meaning that multiple microchips could be fabricated at the same time.
3. Coating protocols were adapted, facilitating effective glioma cell adhesion testing under static and microfluidic conditions in the chip, showed that collagen containing solutions had the best adhesion results.
4. The percentage of cells in microchips after exposure to the flow revealed that 82.9 % of glioma cells stayed adherent to the collagen modified surface, similarly collagen containing mix – 33.8 %.
5. For glioma cells collagen could be used as adhesion promoter, and other solutions can function as matrix or polymer coating compounds.

VILNIUS UNIVERSITY

Life sciences center

Department of Neurobiology and Biophysics

Kamilė Kasperavičiūtė

Master's thesis

Development of a microfluidic chip for studying glioma cell adhesion

SUMMARY

Glioma, a type of brain cancer, poses significant challenges due to its aggressive nature and limited treatment options. Its infiltrative growth pattern and resistance to therapy make it particularly difficult to manage, emphasizing the urgent need for innovative research approaches. Microfluidic chips offer a promising avenue for studying glioma behavior in a controlled environment. With their versatile design and fabrication capabilities, microfluidic chips allow a precise manipulation of fluid behavior at the microscale. Therefore, understanding the importance of cell adhesion within microfluidic chip is crucial, as it plays a pivotal role in the invasive behavior and treatment response.

The fabrication of the microfluidic chip involved a multi-step process, including 3-D printing of master molds, PDMS layer casting, preparation of COC substrates, and injection casting of a photo-curable resin – OSTE. Polycarbonate membranes were placed onto the COC, and the chip was assembled with precise alignment of COC substrates with patterned relief structures. For adhesion modification, microfluidic channels were coated with various solutions, including gelatin 38, gelatin 175, gelatin 300, a mix of gelatin 175/collagen, and collagen.

In the experiment C6 glioma rat cells were used. Prepared solutions were injected into the channels of the microfluidic chips and glioma cells were seeded into the channels afterwards. Over the course of one week, the cells were cultured within the microfluidic environment and imaged using microscopy before and after exposure to fluid flow from the pump. Adhesion behavior of the glioma cells was assessed, with a particular focus on quantifying adherent and non-adherent cells between trials and different adhesion modification methods.

Investigation into microfluidic pump impact on C6 glioma cell adhesion showed variations in cell counts between treatment groups before and after exposure to the microfluidic environment. However, comparison of cell counts between different adhesion modifications revealed that gelatin coatings resulted in decreased adherent cell counts, while collagen and mixed modification methods exhibited higher counts. In conclusion, these results suggest that collagen may be utilized to enhance C6 glioma cell adhesion.

VILNIAUS UNIVERSITETAS

Gyvybės mokslų centras
Neurobiologijos ir biofizikos katedra

Kamilė Kasperavičiūtė
Magistro baigiamasis darbas

Mikrofluidinio lusto sukūrimas gliomos ląstelių adhezijos tyrimams

SANTRAUKA

Glioma, smegenų vėžio rūšis, kelia didelių iššūkių dėl savo agresyvaus pobūdžio ir ribotų gydymo galimybių. Dėl infiltracinio augimo būdo ir atsparumo terapijai ji ypač sunku valdyti, o tai pabrėžia naujoviškų tyrimų metodų poreikį. Mikrofluidiniai lustai yra daug žadantis būdas tirti gliomos elgesį kontroliuojamoje aplinkoje. Dėl savo universalaus dizaino ir gamybos galimybių mikrofluidiniai lustai leidžia tiksliai manipuluoti skysčių elgesį mikroskalėje. Todėl labai svarbu suprasti ląstelių adhezijos svarbą mikrofluidiniame luste, nes ji atlieka pagrindinį vaidmenį invaziniame elgesyje ir gydymo atsake.

Mikrofluidinio lusto gamyba apėmė kelių etapų procesą, įskaitant pagrindinių formų 3-D spausdinimą, PDMS sluoksnių liejimą, COC substratų paruošimą ir foto kietėjančios dervos – OSTE – liejimą. Polikarbonato membranos buvo dedamos tiesiogiai ant COC, o lustas buvo surinktas tiksliai suderinant COC substratus. Adhezijos modifikavimui mikrofluidiniai kanalai buvo padengti įvairiais tirpalais, įskaitant želatiną 38, želatiną 175, želatiną 300, želatinos 175 / kolageno mišinį ir kolageną.

Ekspimente buvo naudojamos C6 gliomos žiurkių ląstelės. Paruošti tirpalai buvo švirkščiami į mikrofluidinių lustų kanalus, kuriuose paruoštos ląstelės vėliau buvo užsėtos. Ląstelės buvo kultivuojamos mikrofluidinėje aplinkoje 7 dienas, po kurių buvo vaizduojamos naudojant mikroskopiją prieš ir po mikrofluidinės pompos. Buvo įvertintas gliomos ląstelių adhezijos elgesys, ypatingą dėmesį skiriant adhezinių ir neadhezinių ląstelių kiekybiniam įvertinimui tarp bandymų ir skirtingų adhezijos modifikavimo metodų.

Mikrofluidinės pompos poveikio C6 gliomos ląstelių adhezijai tyrimas parodė ląstelių skaičiaus skirtumus tarp gydymo grupių prieš ir po mikrofluidinės pompos poveikio. Skirtingų adhezijos modifikacijų ląstelių skaičiaus palyginimas atskleidė, kad želatina sumažino adhezinių ląstelių skaičių, o kolageno ir želatinos 175/kolageno mišinio modifikavimo metodas padidino. Apibendrinant galima pasakyti, kad šie rezultatai rodo, kad kolagenas gali būti naudojamas C6 gliomos ląstelių adhezijai sustiprinti.

ACKNOWLEDGMENTS

I would like to thank my work supervisor dr. Eivydas Andriukonis for the help in the experiments, time in learning new methods, for the provided knowledge, encouragement to be interested and improve, trust throughout the work and patience in preparing the master's thesis and center for physical sciences and technology bioelectrics laboratory head dr. Arūnas Stirkė for the opportunity to work in the laboratory and for the help and advices during experiments.

I would also like to thank dr. Monika Kirsnytė-Šniokė, for the help with microscopy and PhD student Neringa Bakutė, for the provided knowledge about working with cells.

LITERATURE LIST

1. Akther, Fahima, Shazwani Binte Yakob, Nam-Trung Nguyen, and Hang T. Ta. 2020. "Surface Modification Techniques for Endothelial Cell Seeding in PDMS Microfluidic Devices." *Biosensors* 10 (11): 182. <https://doi.org/10.3390/bios10110182>.
2. Amin, Reza, Stephanie Knowlton, Alexander Hart, Bekir Yenilmez, Fariba Ghaderinezhad, Sara Katebifar, Michael Messina, Ali Khademhosseini, and Savas Tasoglu. 2016. "3D-Printed Microfluidic Devices." *Biofabrication* 8 (2): 022001. <https://doi.org/10.1088/1758-5090/8/2/022001>.
3. Babaliari, Eleftheria, Anthi Ranella, and Emmanuel Stratakis. 2023. "Microfluidic Systems for Neural Cell Studies." *Bioengineering* 10 (8): 902. <https://doi.org/10.3390/bioengineering10080902>.
4. Ballabh, Praveen, Alex Braun, and Maiken Nedergaard. 2004. "The Blood-Brain Barrier: An Overview: Structure, Regulation, and Clinical Implications." *Neurobiology of Disease* 16 (1): 1–13. <https://doi.org/10.1016/j.nbd.2003.12.016>.
5. Bhattacharjee, Nirveek, Arturo Urrios, Shawn Kang, and Albert Folch. 2016. "The Upcoming 3D-Printing Revolution in Microfluidics." *Lab on a Chip* 16 (10): 1720–42. <https://doi.org/10.1039/C6LC00163G>.
6. "Biomedical Applications of Microfluidic Devices: Achievements and Challenges - Akbari Kenari - 2022 - Polymers for Advanced Technologies - Wiley Online Library." n.d. Accessed April 26, 2024. <https://onlinelibrary.wiley.com/doi/full/10.1002/pat.5847>.
7. Borda, Eleonora, Danashi Imani Medagoda, Marta Jole Ildelfonsa Airaghi Leccardi, Elodie Geneviève Zollinger, and Diego Ghezzi. 2023. "Conformable Neural Interface Based on Off-Stoichiometry Thiol-Ene-Epoxy Thermosets." *Biomaterials* 293 (February):121979. <https://doi.org/10.1016/j.biomaterials.2022.121979>.
8. Breslauer, David N., Philip J. Lee, and Luke P. Lee. 2006. "Microfluidics-Based Systems Biology." *Molecular BioSystems* 2 (2): 97–112. <https://doi.org/10.1039/B515632G>.
9. Cai, Shuxiang, Chuanxiang Wu, Wenguang Yang, Wenfeng Liang, Haibo Yu, and Lianqing Liu. 2020. "Recent Advance in Surface Modification for Regulating Cell Adhesion and Behaviors." *Nanotechnology Reviews* 9 (1): 971–89. <https://doi.org/10.1515/ntrev-2020-0076>.
10. Campos, Richard Piffer Soares de, Camila Dalben Madeira Campos, Gabriela Brito Almeida, and Jose Alberto Fracassi da Silva. 2017. "Characterization of Off-Stoichiometry Microfluidic

- Devices for Bioanalytical Applications.” *IEEE Transactions on Biomedical Circuits and Systems* 11 (6): 1470–77. <https://doi.org/10.1109/TBCAS.2017.2759510>.
11. Cha, Junghwa, and Pilnam Kim. 2017. “Biomimetic Strategies for the Glioblastoma Microenvironment.” *Frontiers in Materials* 4 (December). <https://doi.org/10.3389/fmats.2017.00045>.
 12. Chambers, Ann F., Alan C. Groom, and Ian C. MacDonald. 2002. “Dissemination and Growth of Cancer Cells in Metastatic Sites.” *Nature Reviews Cancer* 2 (8): 563–72. <https://doi.org/10.1038/nrc865>.
 13. Chen, Xueye, and Jienan Shen. 2017. “Review of Membranes in Microfluidics.” *Journal of Chemical Technology & Biotechnology* 92 (2): 271–82. <https://doi.org/10.1002/jctb.5105>.
 14. Chen, Xueye, Jienan Shen, Zengliang Hu, and Xuyao Huo. 2016. “Manufacturing Methods and Applications of Membranes in Microfluidics.” *Biomedical Microdevices* 18 (6): 104. <https://doi.org/10.1007/s10544-016-0130-7>.
 15. Çökeliler, Dilek. 2013. “Enhancement of Polycarbonate Membrane Permeability Due to Plasma Polymerization Precursors.” *Applied Surface Science* 268 (March):28–36. <https://doi.org/10.1016/j.apsusc.2012.11.136>.
 16. D’Abaco, Giovanna M., and Andrew H. Kaye. 2007. “Integrins: Molecular Determinants of Glioma Invasion.” *Journal of Clinical Neuroscience* 14 (11): 1041–48. <https://doi.org/10.1016/j.jocn.2007.06.019>.
 17. Di Nunno, Vincenzo, Enrico Franceschi, Alicia Tosoni, Lidia Gatto, Stefania Bartolini, and Alba Ariela Brandes. 2022. “Tumor-Associated Microenvironment of Adult Gliomas: A Review.” *Frontiers in Oncology* 12 (July). <https://doi.org/10.3389/fonc.2022.891543>.
 18. Diao, Wenwen, Xuezhi Tong, Cheng Yang, Fengrong Zhang, Chun Bao, Hao Chen, Liyu Liu, et al. 2019. “Behaviors of Glioblastoma Cells in in Vitro Microenvironments.” *Scientific Reports* 9 (1): 85. <https://doi.org/10.1038/s41598-018-36347-7>.
 19. Enders, Anton, Alexander Grünberger, and Janina Bahnemann. 2024. “Towards Small Scale: Overview and Applications of Microfluidics in Biotechnology.” *Molecular Biotechnology* 66 (3): 365–77. <https://doi.org/10.1007/s12033-022-00626-6>.
 20. Errando-Herranz, Carlos, Farizah Saharil, Albert Mola Romero, Niklas Sandström, Reza Zandi Shafagh, Wouter van der Wijngaart, Tommy Haraldsson, and Kristinn B. Gylfason. 2013. “Integration of Polymer Microfluidic Channels, Vias, and Connectors with Silicon Photonic

- Sensors by One-Step Combined Photopatterning and Molding of OSTE.” In *2013 Transducers & Eurosensors XXVII: The 17th International Conference on Solid-State Sensors, Actuators and Microsystems (TRANSDUCERS & EUROSENSORS XXVII)*, 1613–16.
<https://doi.org/10.1109/Transducers.2013.6627092>.
21. Esch, Eric W., Anthony Bahinski, and Dongeun Huh. 2015. “Organs-on-Chips at the Frontiers of Drug Discovery.” *Nature Reviews Drug Discovery* 14 (4): 248–60.
<https://doi.org/10.1038/nrd4539>.
22. Fujii, Teruo. 2002. “PDMS-Based Microfluidic Devices for Biomedical Applications.” *Microelectronic Engineering, Micro- and Nano-Engineering 2001*, 61–62 (July):907–14.
[https://doi.org/10.1016/S0167-9317\(02\)00494-X](https://doi.org/10.1016/S0167-9317(02)00494-X).
23. Furnari, Frank B., Tim Fenton, Robert M. Bachoo, Akitake Mukasa, Jayne M. Stommel, Alexander Stegh, William C. Hahn, et al. 2007. “Malignant Astrocytic Glioma: Genetics, Biology, and Paths to Treatment.” *Genes & Development* 21 (21): 2683–2710.
<https://doi.org/10.1101/gad.1596707>.
24. Gitlin, Leonid, Philipp Schulze, and Detlev Belder. 2009. “Rapid Replication of Master Structures by Double Casting with PDMS.” *Lab on a Chip* 9 (20): 3000–3002.
<https://doi.org/10.1039/B904684D>.
25. Gritsenko, Pavlo G., and Peter Friedl. 2018. “Adaptive Adhesion Systems Mediate Glioma Cell Invasion in Complex Environments.” *Journal of Cell Science* 131 (15): jcs216382.
<https://doi.org/10.1242/jcs.216382>.
26. Gross, Bethany C., Kari B. Anderson, Jayda E. Meisel, Megan I. McNitt, and Dana M. Spence. 2015. “Polymer Coatings in 3D-Printed Fluidic Device Channels for Improved Cellular Adherence Prior to Electrical Lysis.” *Analytical Chemistry* 87 (12): 6335–41.
<https://doi.org/10.1021/acs.analchem.5b01202>.
27. Hajal, Cynthia, Marco Campisi, Clara Mattu, Valeria Chiono, and Roger D. Kamm. 2018. “In Vitro Models of Molecular and Nano-Particle Transport across the Blood-Brain Barrier.” *Biomicrofluidics* 12 (4): 042213. <https://doi.org/10.1063/1.5027118>.
28. Haug, I. J., and K. I. Draget. 2009. “6 - Gelatin.” In *Handbook of Hydrocolloids (Second Edition)*, edited by G. O. Phillips and P. A. Williams, 142–63. Woodhead Publishing Series in Food Science, Technology and Nutrition. Woodhead Publishing.
<https://doi.org/10.1533/9781845695873.142>.

29. Helm, Marinke W van der, Andries D van der Meer, Jan C T Eijkel, Albert van den Berg, and Loes I Segerink. 2016. "Microfluidic Organ-on-Chip Technology for Blood-Brain Barrier Research." *Tissue Barriers* 4 (1): e1142493. <https://doi.org/10.1080/21688370.2016.1142493>.
30. Huang, Qiong, Xingbin Hu, Wanming He, Yang Zhao, Shihui Hao, Qijing Wu, Shaowei Li, Shuyi Zhang, and Min Shi. 2018. "Fluid Shear Stress and Tumor Metastasis." *American Journal of Cancer Research* 8 (5): 763–77.
31. Hwang, Shug-June, Ming-Chun Tseng, Jr-Ren Shu, and Hsin Her Yu. 2008. "Surface Modification of Cyclic Olefin Copolymer Substrate by Oxygen Plasma Treatment." *Surface and Coatings Technology* 202 (15): 3669–74. <https://doi.org/10.1016/j.surfcoat.2008.01.016>.
32. Jena, Rajeeb K., and C. Y. Yue. 2012. "Cyclic Olefin Copolymer Based Microfluidic Devices for Biochip Applications: Ultraviolet Surface Grafting Using 2-Methacryloyloxyethyl Phosphorylcholine." *Biomicrofluidics* 6 (1): 12822–212. <https://doi.org/10.1063/1.3682098>.
33. Jena, Rajeeb, Chee Yue, and Y. Lam. 2012. "Micro Fabrication of Cyclic Olefin Copolymer (COC) Based Microfluidic Devices." *Microsystem Technologies* 18 (February). <https://doi.org/10.1007/s00542-011-1366-z>.
34. Jiang, Qiong, Qing Xie, Chengliang Hu, Zhai Yang, Peizhi Huang, Huifan Shen, Melitta Schachner, and Weijiang Zhao. 2019. "Glioma Malignancy Is Linked to Interdependent and Inverse AMOG and L1 Adhesion Molecule Expression." *BMC Cancer* 19 (1): 911. <https://doi.org/10.1186/s12885-019-6091-5>.
35. Johansson, Bo-Lennart, Anders Larsson, Anette Ocklind, and Åke Öhrlund. 2002. "Characterization of Air Plasma-treated Polymer Surfaces by ESCA and Contact Angle Measurements for Optimization of Surface Stability and Cell Growth." *Journal of Applied Polymer Science* 86 (September):2618–25. <https://doi.org/10.1002/app.11209>.
36. Jong, J. de, R. G. H. Lammertink, and M. Wessling. 2006. "Membranes and Microfluidics: A Review." *Lab on a Chip* 6 (9): 1125–39. <https://doi.org/10.1039/B603275C>.
37. Kamei, Ken-ichiro, Yasumasa Mashimo, Yoshie Koyama, Christopher Fockenber, Miyuki Nakashima, Minako Nakajima, Junjun Li, and Yong Chen. 2015. "3D Printing of Soft Lithography Mold for Rapid Production of Polydimethylsiloxane-Based Microfluidic Devices for Cell Stimulation with Concentration Gradients." *Biomedical Microdevices* 17 (2): 36. <https://doi.org/10.1007/s10544-015-9928-y>.
38. Kaufman, L. J., C. P. Brangwynne, K. E. Kasza, E. Filippidi, V. D. Gordon, T. S. Deisboeck, and D. A. Weitz. 2005. "Glioma Expansion in Collagen I Matrices: Analyzing Collagen

- Concentration-Dependent Growth and Motility Patterns.” *Biophysical Journal* 89 (1): 635–50. <https://doi.org/10.1529/biophysj.105.061994>.
39. Kessler, Laurence, Gilbert Legeay, Arnaud Coudreuse, Patrick Bertrand, Claude Poleunus, Xavier vanden Eynde, Karim Mandes, Pierro Marchetti, Michel Pinget, and Alain Belcourt. 2003. “Surface Treatment of Polycarbonate Films Aimed at Biomedical Application.” *Journal of Biomaterials Science. Polymer Edition* 14 (10): 1135–53. <https://doi.org/10.1163/156856203769231619>.
40. Khalili, Amelia Ahmad, and Mohd Ridzuan Ahmad. 2015. “A Review of Cell Adhesion Studies for Biomedical and Biological Applications.” *International Journal of Molecular Sciences* 16 (8): 18149–84. <https://doi.org/10.3390/ijms160818149>.
41. Kuhn, Phillip, Klaus Eyer, Steffen Allner, Dario Lombardi, and Petra S. Dittrich. 2011. “A Microfluidic Vesicle Screening Platform: Monitoring the Lipid Membrane Permeability of Tetracyclines.” *Analytical Chemistry* 83 (23): 8877–85. <https://doi.org/10.1021/ac201410m>.
42. Leclerc, Eric, Yasuyuki Sakai, and Teruo Fujii. 2003. “Cell Culture in 3-Dimensional Microfluidic Structure of PDMS (Polydimethylsiloxane).” *Biomedical Microdevices* 5 (2): 109–14. <https://doi.org/10.1023/A:1024583026925>.
43. Lee, Nayeon, Jae Woo Park, Hyung Joon Kim, Ju Hun Yeon, Jihye Kwon, Jung Jae Ko, Seung-Hun Oh, et al. 2014. “Monitoring the Differentiation and Migration Patterns of Neural Cells Derived from Human Embryonic Stem Cells Using a Microfluidic Culture System.” *Molecules and Cells* 37 (6): 497–502. <https://doi.org/10.14348/molcells.2014.0137>.
44. Lee, Seung Hwan, Eun Hae Oh, and Tai Hyun Park. 2015. “Cell-Based Microfluidic Platform for Mimicking Human Olfactory System.” *Biosensors & Bioelectronics* 74 (December):554–61. <https://doi.org/10.1016/j.bios.2015.06.072>.
45. Li, Haonan, Guohui Wang, Wenyan Wang, Jie Pan, Huandi Zhou, Xuetao Han, Linlin Su, Zhenghui Ma, Liubing Hou, and Xiaoying Xue. 2021. “A Focal Adhesion-Related Gene Signature Predicts Prognosis in Glioma and Correlates With Radiation Response and Immune Microenvironment.” *Frontiers in Oncology* 11 (September). <https://doi.org/10.3389/fonc.2021.698278>.
46. Li, Xiaoyu, Jinfeng Yao, Xiaojuan Yang, Weidong Tian, and Lei Liu. 2008. “Surface Modification with Fibronectin or Collagen to Improve the Cell Adhesion.” *Applied Surface Science, The First International Symposium on Surfaces and Interfaces of Biomaterials*, 255 (2): 459–61. <https://doi.org/10.1016/j.apsusc.2008.06.105>.

47. Lu, Hang, Lily Y. Koo, Wechung M. Wang, Douglas A. Lauffenburger, Linda G. Griffith, and Klavs F. Jensen. 2004. "Microfluidic Shear Devices for Quantitative Analysis of Cell Adhesion." *Analytical Chemistry* 76 (18): 5257–64. <https://doi.org/10.1021/ac049837t>.
48. Marquet, Colin. 2023. "The Most Used Microfabrication Materials for Microfluidics." Darwin Microfluidics. February 22, 2023. <https://blog.darwin-microfluidics.com/the-most-used-microfabrication-materials-for-microfluidics/>.
49. McKinnon, Chris, Meera Nandhabalan, Scott A Murray, and Puneet Plaha. 2021. "Glioblastoma: Clinical Presentation, Diagnosis, and Management." *BMJ*, July, n1560. <https://doi.org/10.1136/bmj.n1560>.
50. "Microfluidic Calculator." n.d. *Elveflow* (blog). Accessed May 6, 2024. <https://www.elveflow.com/microfluidic-calculator/>.
51. Miller, Kimberly D., Quinn T. Ostrom, Carol Kruchko, Nirav Patil, Tarik Tihan, Gino Cioffi, Hannah E. Fuchs, et al. 2021. "Brain and Other Central Nervous System Tumor Statistics, 2021." *CA: A Cancer Journal for Clinicians* 71 (5): 381–406. <https://doi.org/10.3322/caac.21693>.
52. Mitchell, Michael J., and Michael R. King. 2013. "Computational and Experimental Models of Cancer Cell Response to Fluid Shear Stress." *Frontiers in Oncology* 3 (March). <https://doi.org/10.3389/fonc.2013.00044>.
53. Mofazzal Jahromi, Mirza Ali, Amir Abdoli, Mohammad Rahmanian, Hassan Bardania, Mehrdad Bayandori, Seyed Masoud Moosavi Basri, Alireza Kalbasi, Amir Reza Aref, Mahdi Karimi, and Michael R. Hamblin. 2019. "Microfluidic Brain-on-a-Chip: Perspectives for Mimicking Neural System Disorders." *Molecular Neurobiology* 56 (12): 8489–8512. <https://doi.org/10.1007/s12035-019-01653-2>.
54. Neto, Estrela, Luís Leitão, Daniela M. Sousa, Cecília J. Alves, Inês S. Alencastre, Paulo Aguiar, and Meriem Lamghari. 2016. "Compartmentalized Microfluidic Platforms: The Unrivaled Breakthrough of In Vitro Tools for Neurobiological Research." *Journal of Neuroscience* 36 (46): 11573–84. <https://doi.org/10.1523/JNEUROSCI.1748-16.2016>.
55. Nunes, Pedro S., Pelle D. Ohlsson, Olga Ordeig, and Jörg P. Kutter. 2010. "Cyclic Olefin Polymers: Emerging Materials for Lab-on-a-Chip Applications." *Microfluidics and Nanofluidics* 9 (2): 145–61. <https://doi.org/10.1007/s10404-010-0605-4>.
56. Pardridge, William M. 2005. "The Blood-Brain Barrier: Bottleneck in Brain Drug Development." *NeuroRX* 2 (1): 3–14. <https://doi.org/10.1602/neurorx.2.1.3>.

57. Qazi, Henry, Zhong-Dong Shi, and John M. Tarbell. 2011. "Fluid Shear Stress Regulates the Invasive Potential of Glioma Cells via Modulation of Migratory Activity and Matrix Metalloproteinase Expression." *PLOS ONE* 6 (5): e20348. <https://doi.org/10.1371/journal.pone.0020348>.
58. Raj M, Kiran, and Suman Chakraborty. 2020. "PDMS Microfluidics: A Mini Review." *Journal of Applied Polymer Science* 137 (27): 48958. <https://doi.org/10.1002/app.48958>.
59. Rimsa, Roberts, Artis Galvanovskis, Janis Plume, Felikss Rumnieks, Karlis Grindulis, Gunita Paidere, Sintija Erentraute, Gatis Mozolevskis, and Arturs Abols. 2021. "Lung on a Chip Development from Off-Stoichiometry Thiol–Ene Polymer." *Micromachines* 12 (5): 546. <https://doi.org/10.3390/mi12050546>.
60. Rosser, Julie, Isabel Olmos, Ertl Peter, Florian Jenner, Michaela Purtscher, and Magdalena Shlager. 2015. "Recent Advances of Biologically Inspired 3D Microfluidic Hydrogel Cell Culture Systems." *Herald Journal of Cell Biology and Cell Metabolism* 2 (May). <https://doi.org/10.24966/CBCM-1943/100005>.
61. Roy, Emmanuel, Antoine Pallandre, Bacem Zribi, Marie-Charlotte Horny, François Damien Delapierre, Andrea Cattoni, Jean Gamby and Anne-Marie Haghiri-Gosnet, et al. 2016. "Overview of Materials for Microfluidic Applications." In *Advances in Microfluidics - New Applications in Biology, Energy, and Materials Sciences*. IntechOpen. <https://doi.org/10.5772/65773>.
62. Saharil, Farizah, Carl Fredrik Carlborg, Tommy Haraldsson, and Wouter van der Wijngaart. 2012. "Biocompatible 'Click' Wafer Bonding for Microfluidic Devices." *Lab on a Chip* 12 (17): 3032–35. <https://doi.org/10.1039/C2LC21098C>.
63. Saorin, Gloria, Isabella Caligiuri, and Flavio Rizzolio. 2023. "Microfluidic Organoids-on-a-Chip: The Future of Human Models." *Seminars in Cell & Developmental Biology*, Special Issue: Deconstructing Organs: Decellularized organs, organoids, stem cells niche and engineering new organs, 144 (July):41–54. <https://doi.org/10.1016/j.semcdb.2022.10.001>.
64. Sedo, Aleks, and Rolf Mentlein, eds. 2014. *Glioma Cell Biology*. Vienna: Springer Vienna. <https://doi.org/10.1007/978-3-7091-1431-5>.
65. Shimizu, Toshihiko, Kazuhiko Kurozumi, Joji Ishida, Tomotsugu Ichikawa, and Isao Date. 2016. "Adhesion Molecules and the Extracellular Matrix as Drug Targets for Glioma." *Brain Tumor Pathology* 33 (2): 97–106. <https://doi.org/10.1007/s10014-016-0261-9>.

66. Shoulders, Matthew D., and Ronald T. Raines. 2009. "Collagen Structure and Stability." *Annual Review of Biochemistry* 78 (Volume 78, 2009): 929–58.
<https://doi.org/10.1146/annurev.biochem.77.032207.120833>.
67. Song, Hyunhee, and Hoon Jang. 2023. "The Effect of Gelatin-Coating on Embryonic Stem Cells as Assessed by Measuring Young's Modulus Using an Atomic Force Microscope." *Journal of Animal Reproduction and Biotechnology* 38 (3): 121–30.
<https://doi.org/10.12750/JARB.38.3.121>.
68. Sood, Ankur, Anuj Kumar, Atul Dev, Vijai Kumar Gupta, and Sung Soo Han. 2022. "Advances in Hydrogel-Based Microfluidic Blood–Brain-Barrier Models in Oncology Research." *Pharmaceutics* 14 (5): 993. <https://doi.org/10.3390/pharmaceutics14050993>.
69. To, Naoya, Ippei Sanada, Hikaru Ito, Gunawan S. Prihandana, Shinya Morita, Yoshihiko Kanno, and Norihisa Miki. 2015. "Water-Permeable Dialysis Membranes for Multi-Layered Microdialysis System." *Frontiers in Bioengineering and Biotechnology* 3:70.
<https://doi.org/10.3389/fbioe.2015.00070>.
70. Waheed, Sidra, Joan M. Cabot, Niall P. Macdonald, Trevor Lewis, Rosanne M. Guijt, Brett Paull, and Michael C. Breadmore. 2016. "3D Printed Microfluidic Devices: Enablers and Barriers." *Lab on a Chip* 16 (11): 1993–2013. <https://doi.org/10.1039/C6LC00284F>.
71. Walter, Fruzsina R., Sándor Valkai, András Kincses, András Petneházi, Tamás Czeller, Szilvia Veszelka, Pál Ormos, Mária A. Deli, and András Dér. 2016. "A Versatile Lab-on-a-Chip Tool for Modeling Biological Barriers." *Sensors and Actuators B: Chemical* 222 (January):1209–19.
<https://doi.org/10.1016/j.snb.2015.07.110>.
72. Wang, Da-Yung, Feng-Kuan Chen, Nan-Hua Wang, and Hsin Her Yu. 2007. "Characterization of Hydrogen-Free Diamond-like Carbon Film on COC for Flexible Organic Electro-Luminescence Application." *Thin Solid Films* 516 (2): 293–98.
<https://doi.org/10.1016/j.tsf.2007.07.180>.
73. Westphal, Manfred, and Katrin Lamszus. 2011. "The Neurobiology of Gliomas: From Cell Biology to the Development of Therapeutic Approaches." *Nature Reviews Neuroscience* 12 (9): 495–508. <https://doi.org/10.1038/nrn3060>.
74. Whitesides, George M. 2006. "The Origins and the Future of Microfluidics." *Nature* 442 (7101): 368–73. <https://doi.org/10.1038/nature05058>.
75. Wu, I.-Chi, Je-Wen Liou, Chin-Hao Yang, Jia-Hui Chen, Kuan-Yu Chen, and Chih-Huang Hung. 2023. "Self-Assembly of Gelatin and Collagen in the Polyvinyl Alcohol Substrate and Its

- Influence on Cell Adhesion, Proliferation, Shape, Spreading and Differentiation.” *Frontiers in Bioengineering and Biotechnology* 11 (July). <https://doi.org/10.3389/fbioe.2023.1193849>.
76. Wu, Qirui, Jinfeng Liu, Xiaohong Wang, Lingyan Feng, Jinbo Wu, Xiaoli Zhu, Weijia Wen, and Xiuqing Gong. 2020. “Organ-on-a-Chip: Recent Breakthroughs and Future Prospects.” *BioMedical Engineering OnLine* 19 (1): 9. <https://doi.org/10.1186/s12938-020-0752-0>.
77. Xiao, Minjia, Zhi Jie Xiao, Binbin Yang, Ziwei Lan, and Fang Fang. 2020. “Blood-Brain Barrier: More Contributor to Disruption of Central Nervous System Homeostasis Than Victim in Neurological Disorders.” *Frontiers in Neuroscience* 14:764. <https://doi.org/10.3389/fnins.2020.00764>.
78. Xu, Yonghang, Songshan Zeng, Weikang Xian, Limiao Lin, Hao Ding, Jingjing Liu, Min Xiao, et al. 2021. “Transparency Change Mechanochromism Based on a Robust PDMS-Hydrogel Bilayer Structure.” *Macromolecular Rapid Communications* 42 (1): 2000446. <https://doi.org/10.1002/marc.202000446>.
79. Ye, Xiangdong, Hongzhong Liu, Yucheng Ding, Hansong Li, and Bingheng Lu. 2009. “Research on the Cast Molding Process for High Quality PDMS Molds.” *Microelectronic Engineering*, The Fourth IEEE International Symposium on Advanced Gate Stack Technology (ISAGST 2007), 86 (3): 310–13. <https://doi.org/10.1016/j.mee.2008.10.011>.
80. Zhang, Ran, Duo Zhang, Xingyue Sun, Xiaoyuan Song, Karen Chang Yan, and Haiyi Liang. 2022. “Polyvinyl Alcohol/Gelatin Hydrogels Regulate Cell Adhesion and Chromatin Accessibility.” *International Journal of Biological Macromolecules* 219 (October):672–84. <https://doi.org/10.1016/j.ijbiomac.2022.08.025>.
81. Zhao, Lijun, Weiwei Lan, Xiao Dong, Han Xu, Lili Wang, Yan Wei, Jinchuan Hou, Di Huang, and Weiyei Chen. 2021. “Enhanced Cell Adhesion on Collagen I Treated Parylene-C Microplates.” *Journal of Biomaterials Science, Polymer Edition* 32 (17): 2195–2209. <https://doi.org/10.1080/09205063.2021.1958465>.

Suppl. 1 Comprehensive protocol of microfluidic chip fabrication.

1. Preparation of Cyclic olefin copolymer (COC):

- COC are ultrasonically cleaned (1x10 min in acetone, 1x10 min in isopropanol).
- Dried with compressed air or N₂.
- Before electrode evaporation, the washed COC's are treated with oxygen plasma (for parameters, see Supplement section 6 "Plasma steps").

2. Off-stoichiometry thiol-ene (OSTE) fabrication and preparation for the experiment (approx. 30 min):

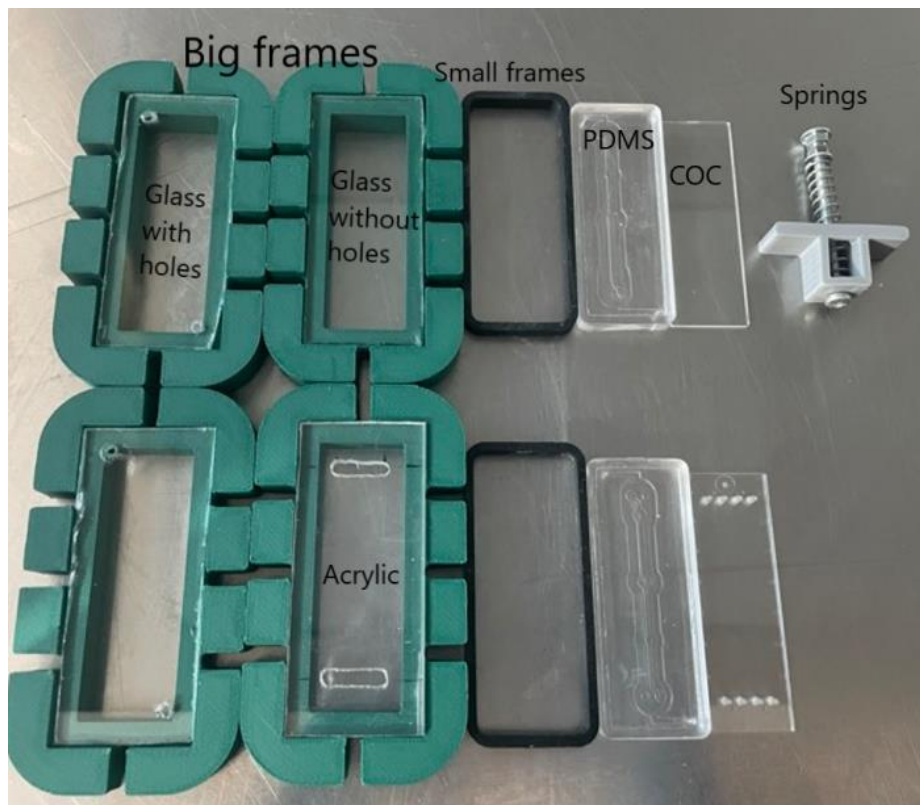
- Approximately 0.5 – 0.7 ml of OSTE is required per COC (OSTE components A and B in a ratio of 1.09:1, respectively).
- OSTE is produced directly into a syringe, mixed and degassed in vacuum chamber until no air bubbles remain.
- Luer adapter is placed on the syringe.
- A thin Polyether ether ketone (PEEK, 1.6 mm diameter) hose (approx. 2 cm long) is placed on the adapter (*TIP – easier with pliers).
- For precise control the syringe is placed in the specific syringe holder (See SFig. 1).
- Foil is placed on the syringe (to protect the OSTE from the light).



SFig. 1. Syringe with prepared OSTE in syringe holder. (Photo courtesy of the author).

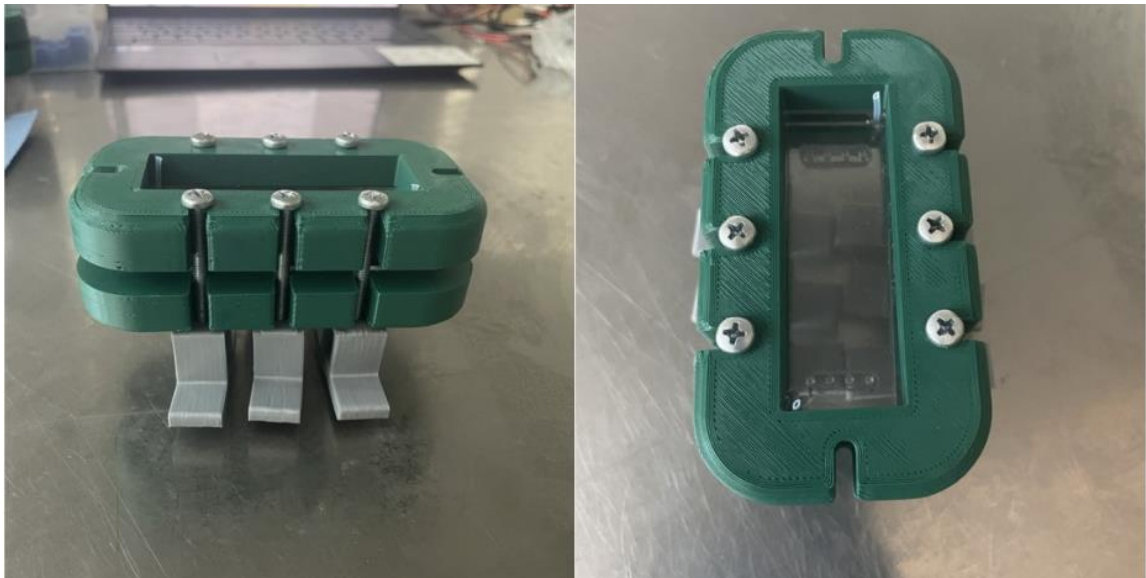
3. Constructing OSTE pouring apparatus:

- Prepare needed parts in advance: 4 big holding frames, two glasses with holes, one glass without holes and one acrylic with specific holes, 2 small frames, top and bottom polydimethylsiloxane molds (PDMS), top and bottom COC and 12 spring clamps (See SFig. 2).



SFig. 2. OSTE pouring apparatus parts. (Photo courtesy of the author).

- Select the appropriate PDMS molds (TOP or BOTTOM).
- Clean the PDMS and all other instruments with isopropanol.
- Place two thin hoses (about 3 cm each) on the dorsal (smooth) side of the PDMS mold. One hose is for the OSTE inlet and the other for the OSTE outlet.
- The PDMS with the hoses is placed on the glass with holes (the hoses are inserted through the holes) and into the first frame.
- Then prepared COC is placed on the PDMS.
- The small frame is placed around the PDMS.
- Second big frame with glass is placed on PDMS (For bottom PDMS – frame with glass without holes; for top PDMS – frame with glass with specific holes for ports).
- 6 springs clamps are placed for reinforcement of apparatus to provide enough clamping force (See SFig. 3).



SFig. 3. OSTE pouring and UV curing apparatus. (Photo courtesy of the author).

4. Prepare UV light (*Exactly in this order):

- Turn on the “Arduino IDE” app on the computer.
- Turn on the extension cord.
- Put white cord in the extension cord.
- USB cord into the computer.
- Black cord into the extension cord.
- Select “Tools” on the app and then “Serial monitor”.
- Select board “Arduino Nano Every COM3”

5. OSTE injection and UV curing (approx. 15 – 20 min):

- Connect the thin entry hose from the syringe to the thick hose and then thick hose to another thin hose that is connected with one end to the PDMS (See SFig. 4).



SFig. 4. Syringe holster connected to constructed apparatus. (Photo courtesy of the author).

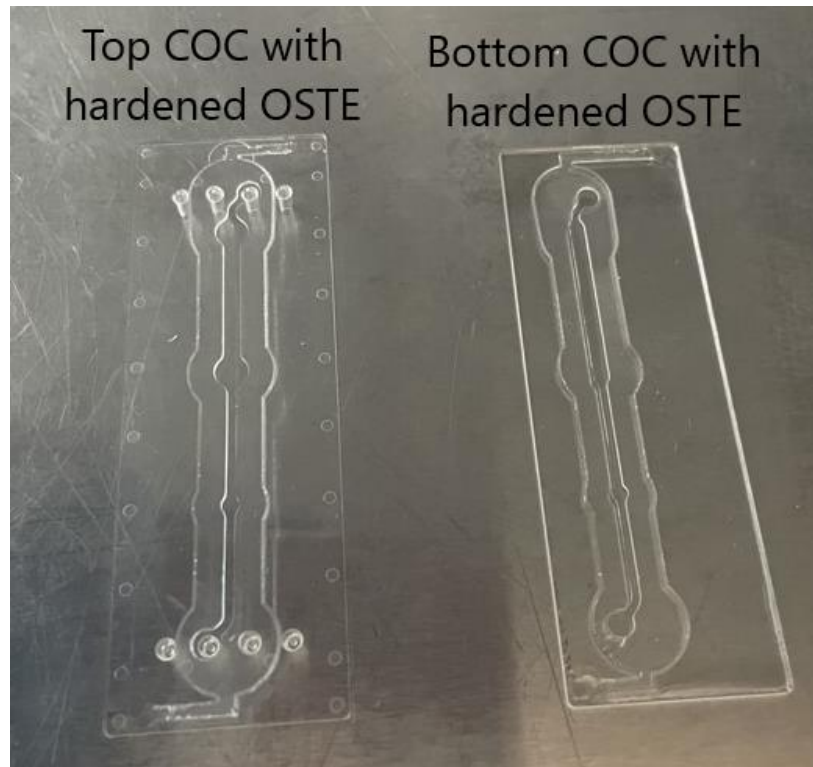
- OSTE is injected until it starts to run through the outlet hose and until the entire surface of the COC is sealed (*CAUTION – leave no air bubbles).
- After injection, half of the inlet and outlet hoses are cut with pliers (See SFig. 5).



SFig. 5. Half of the inlet and outlet hoses are cut with pliers. (Photo courtesy of the author).

- COC with injected OSTE is placed under the UV light and held for 15.5 sec.

- All springs, the frames with glass and remaining hoses are dismantled, then COC carefully separated from the PDMS (See SFig. 6).



SFig. 6. Separated hardened COC with OSTE from the PDMS. (Photo courtesy of the author).

6. Polycarbonate membrane preparation (approx. 10 – 15 min):

- Polycarbonate membrane should be cut in advance with laser according to the shape of the COC.
- Polycarbonate membrane is then placed on the special frame and glued to the corners with an adhesive tape (See SFig. 7).



SFig. 7. Polycarbonate membrane on the special frame. (Photo courtesy of the author).

- Prior to placement on the COC polycarbonate membrane is treated with oxygen plasma. Plasma steps:

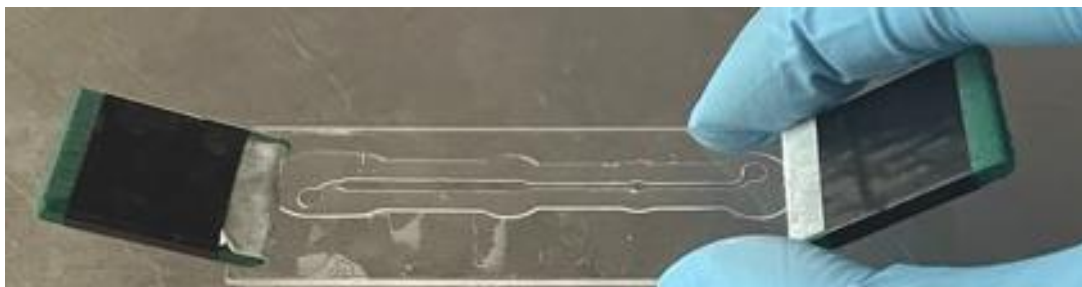
- Turn on O₂ gas
- Press main
- Turn on ventilation
- Place membrane inside
- Close door
- Turn off ventilation
- Press pump
- Set parameters (written below)
- Press generator
- After all - pump off, press ventilation, remove membrane, close door, press pump (for a few seconds), turn off pump, turn off main, turn off O₂ gas (in both – laboratory and gas room)

Parameters:

- O₂ (from 70 – 100 %)
- Power 70 %
- Time - approx. 30 sec

7. Membrane application and construction of the whole chip:

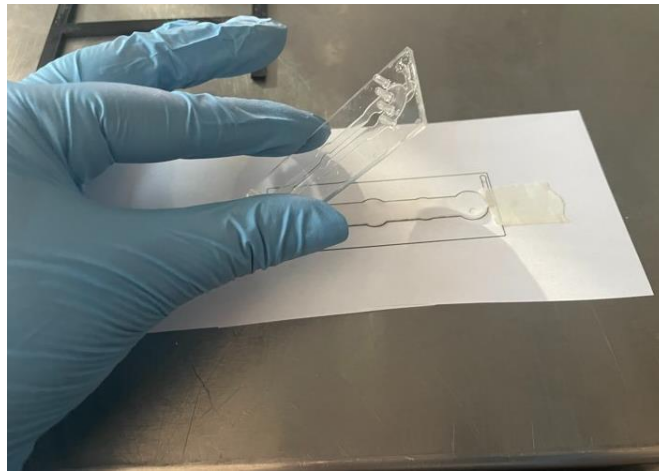
- “Sticky holders” are attached on the prepared top COC with OSTE (It helps to pick COC easier)
(See SFig. 8).



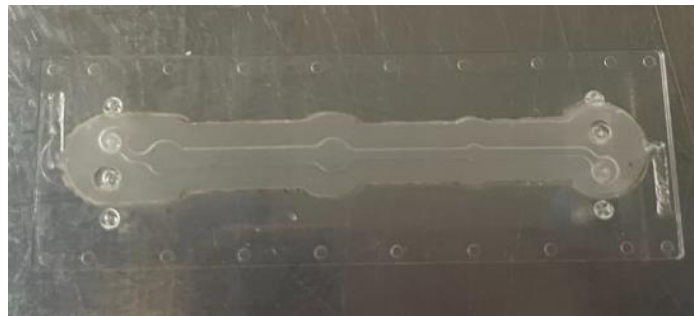
SFig. 8. Sticky holders on COC. (Photo courtesy of the author).

- Polycarbonate membrane is placed on the drawn paper and aligned to the drawn channel.

- Top COC with hardened OSTE is picked with holders and aligned on the membrane (See SFig. 9-10).

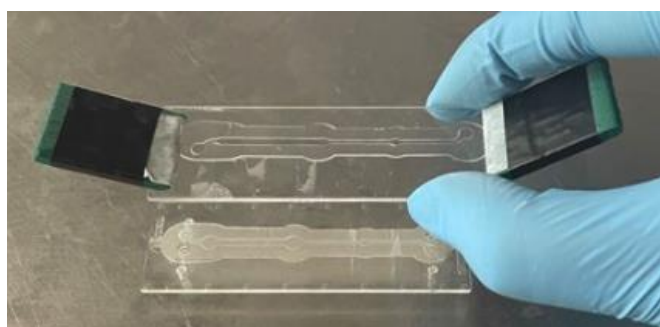


SFig. 9. Polycarbonate membrane is placed on the paper and prepared top COC is placed on top of it. *Sticky holders aren't shown in the photo. (Photo courtesy of the author).

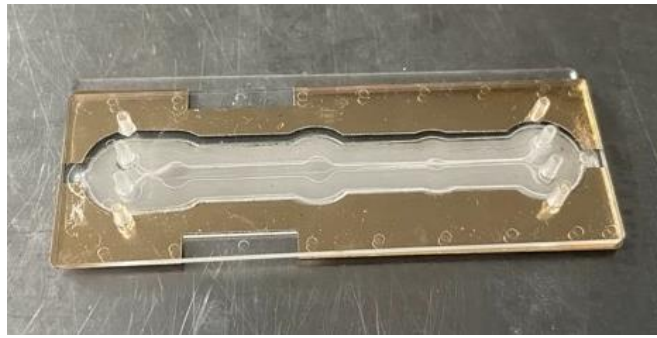


SFig. 10. Top COC with glued polycarbonate membrane. (Photo courtesy of the author).

- Golden paper is put on the top COC with applied membrane (This helps to glue the two COC's evenly and maintain equal pressure and thickness throughout whole area).
- Then COC with membrane and COC without membrane are put together (See SFig. 11-12).



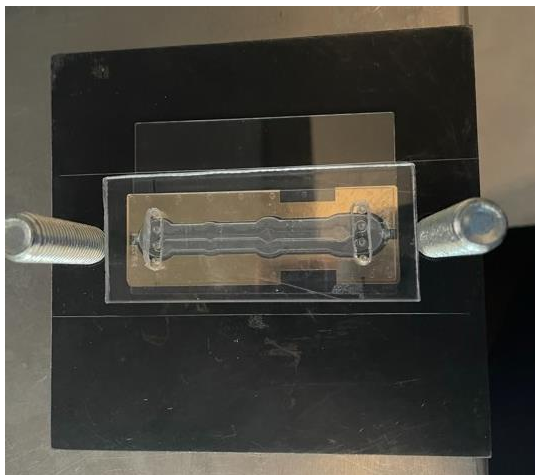
SFig. 11. COC with membrane and COC without membrane are put together *Golden frame isn't shown in the photo. . (Photo courtesy of the author).



SFig. 12. Constructed chip. (Photo courtesy of the author).

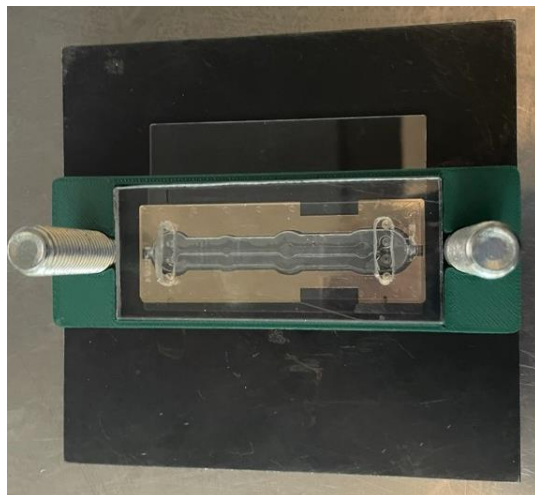
8. Full microchip assembly and clamping:

- Constructed chip is put on the heavy metal.
- Acrylic is put on the constructed chip (See SFig. 13).



SFig. 13. Constructed chip with acrylic on top on the metal. (Photo courtesy of the author).

- Frame is put around the acrylic (It will align it to the middle) (See SFig. 14).



SFig. 14. Constructed chip with acrylic on top and frame. (Photo courtesy of the author).

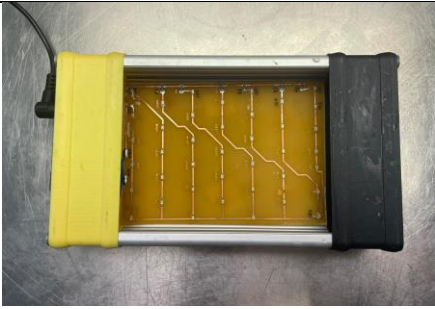
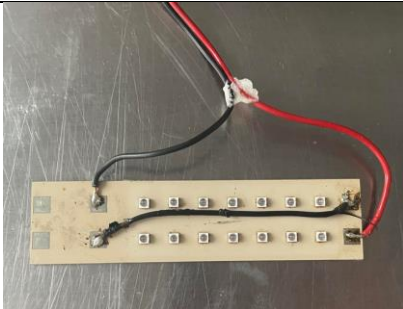
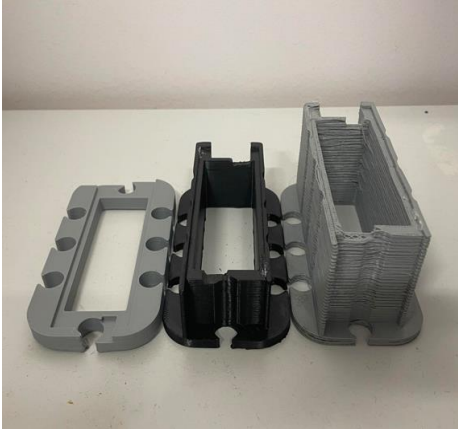

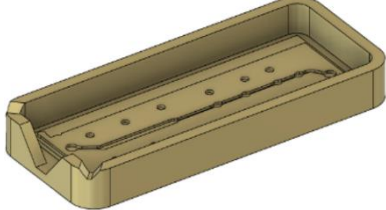
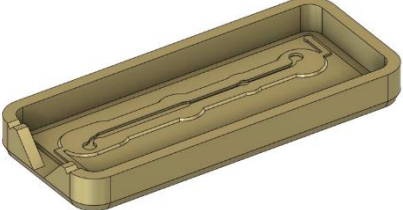
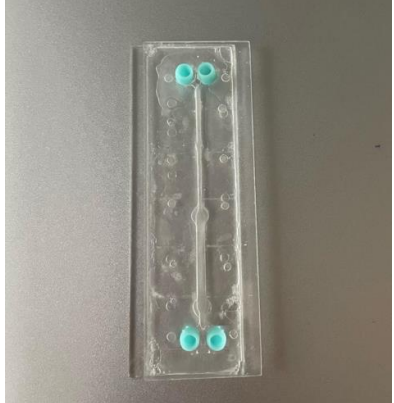

- Another heavy metal is put on top and tighten with screws (See SFig. 15).







SFig. 15. High pressure clamping and curing jig assemble. (Photo courtesy of the author).

- The whole constructed chip is cured for at least 4 hours (or overnight) in 60°C temperature.
After curing – everything is dismantled.

Suppl. 2 Initial and updated materials for microfluidic chip fabrication.

	Initial materials	Updated materials	Outcome
UV light source			<p>The upgraded UV light source features a high-powered LED module with an optical power output of 1 W per single LED, significantly enhancing the efficiency of the curing process and reducing it 5 times.</p>
UV light holder			<p>Multiple sizes of UV light holders were tested, which often resulted in inconsistent distances and variable curing quality. Incorporation of standardized tabs between lights removed UV light interference effects, ensured a consistent and optimal distance from the chip, improving the uniformity of UV exposure and curing.</p>
PDMS mold design			<p>Incorporating relief angles facilitates easier removal of PDMS from the printed master mold and OSTE from PDMS</p>
Luer ports			<p>The incorporation of pre-fabricated COC substrates with integrated ports has significantly improved the consistency and reliability of the microfluidic chips, reducing the time involved in manual assembly and enhancing overall robustness.</p>

<p>Spring-based clamping system</p>					<p>Increased spring density achieved more uniform compression throughout the surface for enhanced fabrication precision.</p>
<p>OSTE injection</p>					<p>A syringe holder was developed to ensure more uniform dispensing of OSTE, enhancing the consistency of injection volumes.</p>